# Plant-Wide Anti-Slug Control for Offshore Oil and Gas Processes

Pedersen, Simon

*DOI (link to publication from Publisher):*
10.5278/vbn.phd.engsci.00183

*Publication date:*
2016

*Document Version*
Publisher's PDF, also known as Version of record

# PLANT-WIDE ANTI-SLUG CONTROL FOR OFFSHORE OIL AND GAS PROCESSES

**BY**
**SIMON PEDERSEN**

DISSERTATION SUBMITTED 2016

AALBORG UNIVERSITY
DENMARK

# Plant-Wide Anti-Slug Control for Offshore Oil and Gas Processes

Ph.D. Dissertation

Simon Pedersen

Dissertation submitted September, 2016

Dissertation submitted: September, 2016

PhD supervisor: Assoc. Prof. Zhenyu Yang
Aalborg University

PhD committee: Professor Rafal Wisniewski (chairman)
Aalborg University

Professor Bjarne Foss
Norwegian University of Science and Technology

Dr. Yi Cao
Cranfield University

PhD Series: Faculty of Engineering and Science, Aalborg University

ISSN (online): 2246-1248
ISBN (online): 978-87-7112-796-6

Published by:
Aalborg University Press
Skjernvej 4A, 2nd floor
DK – 9220 Aalborg Ø
Phone: +45 99407140
aauf@forlag.aau.dk
forlag.aau.dk



Printed in Denmark by Rosendahls, 2016

# Abstract

In offshore Oil & Gas production processes the undesired severe slug flow regime can be present. The negative impact of severe slug is crucial to the production rate and process safety. In this work, the severe slugs which occur in the well-pipeline-riser system are experimentally and theoretically investigated though mathematical modeling, laboratory experiments, control system design and analysis, numerical simulations and laboratory implementations.

In general, this thesis studies the modeling and control of slugging flows which can occur in offshore well-pipeline-riser systems, from both theoretical and experimental perspectives. Some typical control-oriented mathematical models are reviewed and examined. Some extensions have been proposed for improving the model accuracies. The choice of control structure is analyzed based on the Input-Output (IO) controllability concept. All the respective studied measurements give better results than the frequently used riser topside pressure ($P_t$). A supervisory self-learning control strategy is developed and the results show that the decision making based on the supervisor drives the system close to the closed-loop bifurcation point, but a faster control scheme can reduce the settling time significantly. A number of anti-slug control strategies are proposed, where the robust control solution shows the best potential in both anti-slug control and production rate improvement. Simulation results show that control solutions with the riser bottom pressure $P_b$ performs better than the ones developed for $P_t$. Furthermore, an alternative transmitter is experimentally investigated for online slug detection and monitoring. The transmitter is an Electrical Resistance Tomography (ERT) sensor measuring the electrical resistance over the cross-area section of the transportation channel. The results show that the transmitter can be a good alternative to conventional measurements if the oil-to-water ratio is low and the fluids are well-mixed. The severe slug's influence on the downstream separation process is examined. It is confirmed that the riser-induced slugs entering the gravity separator has significant impact on the pressure-drop-ratio (PDR) controller's tracking performance on the de-oiling hydrocyclone.

Most of this thesis's contributions have been experimentally examined

and validated. Some problems and techniques still need further investigations in the future, for example, automatic generations of slug models and corresponding control solutions, with respect to the fact that the slug characteristics of the individual installations in offshore productions can differ significantly from each other.

# Synopsis

I offshore olie og gas produktionsprocesser kan den uønskede alvorlige slug strømningstype være tilstedeværende. Den negative påvirkning af alvorlig slug er vital for produktionsraten og processikkerheden. I dette arbejde vil de alvorlige slugs, som opstår i brønd-rørledning-stigrør systemer, blive undersøgt gennem matematisk modellering, laboratorieforsøg, kontrolsystemdesign og -analyse, numeriske simuleringer og laboratorieimplementeringer.

Generelt studerer denne afhandling modellering og kontrol af slugstrømninger, som opstår i offshore brønd-rørledning-stigrør systemer, fra både teoretiske og eksperimentelle perspektiver. Nogle af de typiske kontrolorienterede matematiske modeller er gennemgået og inspiceret. Nogle udvidelser er blevet foreslået for at forbedre model-nøjagtighederne. Valget af kontrolstruktur er analyseret baseret på Input-Output (IO) controllability-konceptet. Alle de respektive studerede målinger giver bedre resultater end den hyppigt anvendte stigrørs toptryk ($P_t$). En overvågnings-selvlærende kontrolstrategi er udviklet og resultaterne viser at beslutningsvalgene baseret på overvågningen, kører systemet tæt på den lukkede løkkes bifurkationspunkt, men at en hurtigere kontrolplan kan reducere stabiliseringstiden signifikant. Et antal af anti-slug kontrolstrategier er foreslåede, hvor den robuste kontrolløsning viser det bedste potentiale for både anti-slug kontrol og forbedring af produktionsrate. Simuleringsresultater viser at kontrolløsningerne med stigrørs bundtryk ($P_b$) præsterer bedre end løsningerne med $P_t$. Ydermere er en alternativ transmitter eksperimentelt undersøgt som online slug-detektion og -overvågning. Transmitteren er en Elektrisk Modstandstomografi (ERT) sensor, som måler det elektriske modstand over en tværsnitssektion af en transportkanal. Resultaterne viser at transmitteren kan være et godt alternativ til konventionelle målemetoder, hvis olie-til-vand forholdet er lavt og væskerne er velblandet. Den alvorlige slugs indflydelse på nedstrøm-separeringsprocessen er undersøgt. Det er bekræftet at de stigrør-skabte slugs som går ind i tyngdekrafts-separatoren har signifikant påvirkning på "tryk-tab-forhold (PDR)"-styringens forfølgelsespræstation på afolie- hydrocyklonen.

Det meste af afhandlingens bidrag er blevet eksperimentelt undersøgt og

valideret. Nogle problemer og teknikker mangler stadig at bliver udforsket og valideret i fremtiden, for eksempel automatisk generering af slugmodeller og tilsvarende kontrolløsninger, med hensyn til det faktum at slugkarakteristika af de individuelle installationer i offshore-produktioner kan varierer signifikant fra hinanden.

# Contents

# Thesis Details

| | |
|---|---|
| **Thesis Title:** | Plant-Wide Anti-Slug Control for Offshore Oil and Gas Processes |
| **Ph.D. Student:** | Simon Pedersen |
| **Supervisor:** | Assoc. Prof. Zhenyu Yang, Aalborg University |

The main body of this thesis consist of the following papers.

[A] Simon Pedersen, Petar Durdevic and Zhenyu Yang, "Review of Slug Detection, Modeling and Control Techniques for Offshore Oil & Gas Production Processes", *Proceedings of the 2nd IFAC Workshop on Automatic Control in Offshore Oil and Gas Production*, vol. 48, no. 6, pp. 89—96, 2015.

[B] Simon Pedersen, Petar Durdevic and Zhenyu Yang, "Challenges in Slug Modeling and Control for Offshore Oil and Gas Productions: A Review Study", *In press at International Journal of Multiphase Flow*, 2016.

[C] Simon Pedersen, Petar Durdevic, Kasper Stampe, Sandra Lindberg Pedersen and Zhenyu Yang, "Experimental Study of Stable Surfaces for Anti-Slug Control in Multi-phase Flow," *International Journal of Automation and Computing, Special Issue on Innovative Applications of Automation and Computing Technology*, vol. 13, no. 1, pp. 81–88, 2016.

[D] Simon Pedersen, Christian Mai, Leif Hansen, Petar Durdevic and Zhenyu Yang, "Online Slug Detection in Multi-phase Transportation Pipelines Using Electrical Tomography", *Proceedings of the 2nd IFAC Workshop on Automatic Control in Offshore Oil and Gas Production*, vol. 48, no. 6, pp. 159–164, 2015.

[E] Simon Pedersen, Petar Durdevic and Zhenyu Yang, "Learning Control for Riser-slug Elimination and Production-rate Optimization for an Offshore Oil and Gas Production Process", *Proceedings of the 19th World Congress of the International Federation of Automatic Control*, pp. 8522–8527, 2014.

[F] Simon Pedersen, Esmaiel Jahanshahi, Zhenyu Yang and Sigurd Skogestad, "Comparison of Model-based Control Solutions for Severe Riser-induced Slugs", *Submitted to Control Engineering Practice*, 2016.

[G] Simon Pedersen, Petar Durdevic and Zhenyu Yang, "Influence of riser-induced slugs on the downstream separation processes", *Submitted to International Journal of Multiphase Flow*, 2016.

In addition to the main papers, the following project-relevant publications have also been made.

[1] Zhenyu Yang, Simon Pedersen and Petar Durdevic, "Cleaning the Produced Water in Offshore Oil Production by Using Plant-wide Optimal Control Strategy", *Proceedings of the OCEANS'14 MTS/IEEE Conference*, 2014.

[2] Petar Durdevic, Leif Hansen, Christian Mai, Simon Pedersen and Zhenyu Yang, "Cost-Effective ERT Technique for Oil-in-Water Measurement for Offshore Hydrocyclone Installations", *Proceedings of the 2nd IFAC Workshop on Automatic Control in Offshore Oil and Gas Production*, vol.48, no.6, pp. 147—153, 2015.

[3] Petar Durdevic, Simon Pedersen, Mads Bram, Dennis Hansen, Abdiladif Hassan and Zhenyu Yang, "Control Oriented Modeling of a Deoiling Hydrocyclone", *Proceedings of the 17th IFAC Symposium on System Identification*, vol.48, no.28, pp. 291—296, 2015.

[4] Mads Bram, Abdiladif Hassan, Dennis Hansen, Petar Durdevic, Simon Pedersen and Zhenyu Yang, "Experimental Modeling of a Deoiling Hydrocyclone System", *Proceedings of the 20th International Conference on Methods and Models in Automation and Robotics*, pp. 1080–1085, 2015.

[5] Petar Durdevic, Simon Pedersen and Zhenyu Yang, "Evaluation of OiW Measurement Technologies for Deoiling Hydrocyclone Efficiency Estimation and Control", *Proceedings of OCEANS MTS/IEEE*, 2016

[6] Petar Durdevic, Simon Pedersen and Zhenyu Yang, "Efficiency Control in Offshore De-oiling Installations", *Submitted to Computers and Chemical Engineering*, 2016

In addition to the project-related papers, the following publications have also been made.

[7] Zhenyu Yang, Simon Pedersen and Petar Durdevic "Control of Variable-Speed Pressurization Fan for an Offshore HVAC System", *Proceedings of the 2014 IEEE International Conference on Mechatronics and Automation (ICMA)*, pp. 458–463, 2014.

[8] Petar Durdevic, Simon Pedersen and Zhenyu Yang, "Modeling Separation Dynamics in a Multi-Tray Bio-Ethanol Distillation Column", *Proceedings of the 2015 IEEE International Conference on Mechatronics and Automation (ICMA)*, pp. 1349–1354, 2015.

This thesis has been submitted for assessment in partial fulfillment of the PhD degree. The thesis is based on the submitted or published scientific papers which are listed above. Parts of the papers are used directly or indirectly in the extended summary of the thesis. As part of the assessment, co-author statements have been made available to the assessment committee and are also available at the Faculty. The thesis is not in its present form acceptable for open publication but only in limited and closed circulation as copyright may not be ensured.

# Preface

This thesis is submitted as a collection of papers in fulfillment of the requirements for the degree of Doctor of Philosophy at the Department of Energy Technology, Aalborg University, Denmark. The work has been carried out in the Department of Energy Technology, Aalborg University, Esbjerg Campus, in the period from August 2013 to July 2016 under the supervision of Associate Professor Zhenyu Yang. During the project period I have been a visiting researcher in the Department of Chemical Engineering, Norwegian University of Science and Technology (NTNU), Norway, from October 2015 to December 2015. This work has been partially supported by the Innovation Fund Denmark, Mærsk Oil and Rambøll Oil & Gas through the "Plant-wide De-oiling of Produced Water using Advanced Control (PDPWAC)" Project (No. 95-2012-3).

I would like to thank all colleagues from the Department of Energy Technology, Aalborg university and Department of Chemical Engineering, NTNU for providing resourceful, positive and delightful research environments. From both places, I have enjoyed gaining knowledge with talented research groups and appreciated the open environments where ones views on any task never are regarded negligible.

I would especially like to thank my supervisor Zhenyu Yang for his constant positive support, our many valuable discussions and for also being an excellent friend. I would like to thank my office mate Petar Durdevic and my project colleagues Christian Mai, Kasper Jepsen and Leif Hansen for being brilliant researchers who were always there when I needed help. Also a big thanks to my friends and former colleagues Lasse Hansen and Jakob Biltoft for contributing to the pre-investigations for the PhD work, thus giving me the motivation to begin the PhD work.

Lastly, I would like to express my gratitude to my family and friends, especially my girlfriend, parents and siblings for their endless support. They were a source of constant motivation in times of need.

Simon Pedersen
Aalborg University, September 10, 2016

# Part I

# Introduction

# Introduction

*This chapter presents the context, the problem, the approach and the general outline of the thesis.*

## 1 Context and Motivation

Gas-liquid multi-phase flow in a pipeline can take a large number of possible shapes with subject to the specific flow conditions. However, these shapes can be classified according to different types of fluid distributions; commonly called flow patterns or regimes [9]. The slug flow is a common flow pattern in the oil & gas production processes. It exists when gas pockets fill up the entire pipeline cross area. The slugs can be induced by the physical construction, both in the horizontal and vertical pipelines, due to transient response related to pigging, start-up, shut-down or changes in the set-points of pressures or flow rates [10, 11]. The severity of the slugs heavily depends on the sizes of the gas pockets and how much the pressure, temperature and flow rate oscillates in the system. Some of the most severe slugs are induced by gas-lifting casing-heading in vertical wells [12,13] or by gas-holdup in vertical risers [14]. The severe slugs are characterized by significant amplitude fluctuations in the pressures and flow rates, due to gas accumulation in the riser base for the riser-induced slugs [15] and in the casing for the well-induced slugs [16, 17].

In offshore oil & gas processes severe slugs can occur in the transportation pipeline systems, prior to the separator of the multi-phase fluids. Figure 1 illustrates a typical transportation well-pipeline-riser system. The oil & gas reservoir is connected to the well inlet and the outlet of the riser is connected to a 3-phase separator. Thus, the well-pipeline-riser process links the reservoir to the separation platform. There exist huge economic benefits in eliminating or just reducing the severe slugs in this process as it ultimately increases the fuel recovery from the reservoir [18].

Nearly the entire well-pipeline-riser is located subsea. All installation and maintenance of the subsea equipment are both very expensive and time-

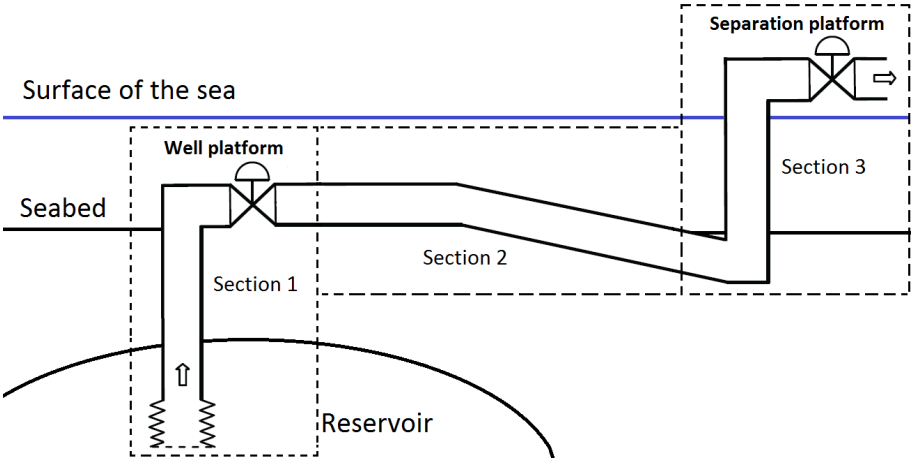


**Fig. 1:** Figure from Paper B. An illustration of a typical well-pipeline-riser system, which consists of: (i) The well, (ii) the transportation pipeline, and (iii) the riser.

consuming, hence the amount of equipment is very limited before reaching the separation platform [19]. This challenges the operators monitoring the system, as the lack of sensors limits the overview of the plant and the lack of actuators reduces the freedom to manipulate the process.

The remainder of this chapter is organized as follows: First we describe the motivation for eliminating well- and riser-induced slugs with focus on applying intelligent anti-slug control. Then a brief description of the problem formulation and motivation behind each paper is carried out.

## 1.1 Motivation for eliminating severe slugs

The occurrence of severe slugs induced by either wells or risers have negative impact on the production facilities in several ways [20,21]. Some of the main disadvantages are: The liquid blowouts from the slug cycles can give liquid overflows and increase the pressures higher than the safety threshold in the separators [22,23] which also affects the performance of the downstream separation process [24], high frictional pressure drops in the pipelines which increases shear stressing to the wall [20], overloading on the gas compressors, reduction of the production rate [15], production slop from flaring of the natural gas, increased corrosion [25–27] and extra fatigue loads from the repeating oscillating pressures [20].

Thus, the slug elimination solutions developed examined in this thesis will not only be evaluated based on whether the severe slug is eliminated, but also on:

- The cost and convenience of implementation.
- The operating production rate.
- The influence to the separation processes.
- The robustness of the solution.

If a solution can satisfy all four bullet points at an acceptable level while eliminating the severe slug, it is then considered suitable for applying in reality.

## 1.2 Motivation for anti-slug control

Hardware-based slug elimination is often referred to as flow conditioners [28], which describe passive methods to eliminate the slug as no actuator is acting on the system. It is a common approach and can be effective in reducing the severe slug regime's region on flow maps [29]. Flow conditioners can be designed as helical pipelines [30], wavy pipelines [28, 31, 32], curved pipeline bends [33], sidestream vertical pipelines for gas to create self-gas lifting mechanisms [34,35], venturi-shaped pipelines with nozzle sections [36,37], permanently choking valves to fixed positions [38], homogenizers to homogenize the multi-phase fluids to foam [39] or as slug catchers [40]. The flow conditioners most commonly applied are the slug catchers as they have a simple design and can be located topside above sea level. However, they are limited by the buffer volume and thus it often cannot handle severe slugs with large amplitudes and low frequencies. The foam homogenizer causes issues for the downstream separation process. The other listed flow conditioners either only suppress and/or reduce the occurrence (eg. reducing flow maps' slug regime regions) of severe slugs or heavily decrease the production rate. However the biggest limitations for all existing flow conditioners are the expenses for the installation, maintenance and physical space requirements. These hardware-based expenses could be significantly reduced by applying some alternative anti-slug solutions, for example some software-based control solution by applying feedback control to already existing actuators with information from already existing transmitters.

In the recent years feedback control has been a common approach to eliminate the severe slugs [36,37]. Two different approaches are traditionally used as the manipulated variable, respectively: Manipulation of a topside choke valve [41–44] or by applying gas-lifting [45–48]. Both of these manipulated variables can exist on both wells and risers. Gas compressors supplies the gas for injection and have limited capacity, which can be a constraint for the expected performance. For example, the compressors system may not always be able to fulfill the tracking performance of the gas-injection setpoints, especially when relatively large amounts of injected gas is needed to

stabilize the flow [17, 38]. In many cases the topside choke valves at wellhead and riser top are the only available actuators for anti-slug control in a well-pipeline-riser process. The main disadvantage of choking a valve to stabilize the flow is the reduction of production rate because of the increased back pressure. Hence, several studies has aimed for eliminating the severe slug while keeping the operation at large valve openings [42, 49]. However, operating at large valve openings reduces the closed-loop systems' robustness against input/parametric system disturbances [50]. This has motivated this thesis' examination of controllers with acceptable performance and good disturbance rejection.

## 1.3 Motivation for paper A and B

Paper A gives a review of the concepts of slugs, slug criteria, modeling and elimination. Paper B gives a detailed overview of the challenges which arises when severe slug flow occurrs in the well-pipeline-riser sections. Both papers aim to give an all-around understanding of the severe slugs, its limitations, how to handle it and what the consequences are. These papers are expected to lay out good starting points for process and control engineers in the area, but also strives towards predicting the tendencies in the area of slug detection, modeling and control, to help experienced people in the field.

Other review studies examining slug flows can be found in [51–56].

## 1.4 Motivation for paper C

Paper C is an extended version of the paper documented in [57]. In Paper C the recreation of the severe slug flow is examined based on experiments on an economic lab-sized test rig developed in [58]. The work focuses on how to emulate the physics behind severe slugs by creating an open-loop analysis of the flow regimes, where traditional flow and bifurcation maps are created. Based on the attained data, a new-developed 3D flow map concept is created with color to indicate the 4th dimension for combining the information gained from the flow and bifurcation maps into one new manipulatable flow map. The stable surface is mapped to indicate the switching between slugging and non-slugging flows. By adding this extra dimension represented by the manipulated variable (choke valve opening degree), the manipulatable flow map can help operators getting an improved plant overview by combining the information from the traditional maps and the corresponding characteristics induced by the variable choking.

## 1.5 Motivation for paper D

It is highly debated which transmitters are best for slug monitoring and control [59]. Paper D examines a self-developed transmitter for monitoring the severe slugs in pipelines. The proposed transmitter is an Electrical Resistance Tomography (ERT) sensor, which can track the cross-section electrical resistance with 12 probes in a nearly real-time manner. The developed sensor is tested on a stand-alone test facility has been constructed with a relatively short horizontal pipeline, a compressor and a pump for emulating the riser-induced multi-phase slugs. The ERT's average cross-section electrical resistance proved to provide consistent information with flow measurements, and the paper concludes that the ERT technique can be a good alternative to the available measurements used in the offshore industry.

There exist relevant literature for applying ERT and ECT for other applications: Online monitoring of air cores in hydrocyclones using ERT [60], using ECT for foam processes [61] and online monitoring of oil-water separation in hydrocyclones [62].

## 1.6 Motivation for paper E and F

It can be challenging finding the highest achievable closed-loop bifurcation point with an anti-slug control scheme. For this reason adaptive references can be useful for improving the production rate while staying within the stable flow region [49]. Paper E examines the development of a learning controller which can adapt to slow condition changes. The controller is based on a supervisor which is a decision maker for a switching PID control scheme. The advantage of this adaption is the controllers' flexibility for handling process and condition changes. However, the disadvantages of the learning strategy are the slow convergence rate and the corresponding lack of ability to compensate for high frequency disturbances and rapid changes in the running conditions.

An anti-slug controller's robust performance is important due to the uncertain and varying running condition on real plants. Paper F considers low-dimensional and OLGA modeling, Input-Output (IO) controllability analysis based on the low-dimensional model, controller development and the corresponding simulation results. The results show that a robust controller can improve the robustness without losing much of the nominal performance. Furthermore, Paper F concludes that the riser bottom pressure ($P_b$) is preferred over the topside pressure ($P_t$) for SISO control schemes, when a topside choke valve is applied as the manipulated variable. The examined control solutions with $P_t$ as controlled variable can still operate above the open-loop bifurcation point, but not with large valve openings.

Similar IO controllability analysis has been examined in [50] and the linear

controller designs have been suggested in [63].

## 1.7 Motivation for paper G

The presence of riser-induced slugs is believed to play a significant role to the upstream separation processes. Paper G investigates the dynamic correlation between severe riser-induced slug flow and the traditional separation process downstream the riser. The paper experimentally investigates the influences of several flow and anti-slug control scenarios to the downstream separation process consisting of a 3-phase gravity separator and a water-oil de-oiling hydrocyclone. The paper concludes that the separation performance is sensitive to the flow oscillations, when the traditional gravity separator's gas pressurization, water level and the hydrocyclone's pressure-drop-ratio (PDR) controllers are implemented. Here, especially the PDR controller is significantly challenged with the presence of severe slugs. It is experimentally confirmed that an anti-slug controller can improve the separation performance significantly, with subject to water level and PDR reference tracking, while also keeping an acceptable production rate.

# 2 Methodology

In this chapter a brief review of the slug identification, modeling, elimination and control will be presented. The main ideas of anti-slug control used throughout the thesis originate from these concepts. Hence, the relevant concepts from the theory are reviewed. In particular slug modeling and control will be examined. Detailed review documentation can be found in paper A and B.

## 2.1 Review of slug modeling

Slug modeling is a challenging task, as the slug flow has some chaotic characteristics [64, 65]. In recent years commercial software products, such as OLGA [66] and LedaFlow [67, 68], have been developed for simulating the flow patterns in the multi-phase transportation pipelines. They can successfully predict severe slug in some relatively simple cases but also equivalently poor in some complicated cases [69]. Nevertheless, the commercial software tools are still widely applied in the offshore oil & gas industry as they currently are the preferred tools for estimating the different flow patterns.

Process and control engineers prefer simple low-dimensional models for designing control schemes. Hence, several studies have developed low- dimensional anti-slug control-oriented models both for well and riser slugs, respectively [46,70–77]. In [71] a detailed model comparison was was carried out benchmarking against OLGA simulation data, where it was concluded

that the two respective models examined in [71] and [75] were the two best models when complexity and accuracy were taken into account.

Paper E is examining a model based on [75,76] and in paper F the model is extended from the model developed in [44,71,77].

## 2.2 Review of anti-slug control

The topside choking and gas-lifting represent the two typical manipulated variables preferred for anti-slug control strategies, respectively [42]. The selection of controlled variable is still an open discussion in the industry, due to the large amount of measurement types and possible installation locations. In [44,50,78] Input-Output controllability analysis on low-dimensional model were carried out for two cases: A well-pipeline-riser and an oil well. For both cases the bottomhole/riser-base pressure was the preferred controlled variable for topside valve control. The topside pressure transmitter was considered a bad choice due to the right half plane (RHP) zeroes and the related inverse system response. If only topside measurements were considered, then the topside flow meter was suggested as a better choice. However, in [76] the performance of an observer controller using the topside pressure measurement did not seem to be influenced by the existing RHP zero, which contradicted the conclusion from [79]. In a similar way the work examined in [42] was able to stabilize the flow with large valve openings only using the topside pressure measurement. Thus, no consistent unity conclusion can be given for picking the best single measurement as controlled variable.

It is commonly agreed that if only common topside transmitters are available on an offshore installation the combination of a mass flow meter and a pressure transmitter are preferred [50,59,78,79]. The work in [59,80,81] also proposed various combinations for cascade control of topside measurements.

### 2.2.1 Topside choking

Choking the topside control valve has proven to be one of the most successful methods for taming the severe slugs in both wells and risers [38,41,82–84]. When a valve is choked, the pressure drop across the choke valve increases. This reduces the velocities of the fluids in the riser and prevents the slug's gas tail from penetrating the riser base at once, which will result in a shift in the flow regime to bubbly gas flow [85].

Observed-based methods have been used for eliminating the slug when there is a lack of transmitters installed [86–91]. However, these methods are limited by the accuracy of the models, which often lack robustness. In [92] feedback linearization was applied for a developed control scheme, where the performance also heavily relies on the accuracy of the applied model in the control scheme.

The ultimate objective for all of the controllers is to operate at large valve openings to improve the production rate while avoiding the severe slug regime [43,93,94]. This can be challenging, as the increased operational opening reduces the closed-loop system's stability [50]. Thus, in [49] a supervisor aims for driving the closed-loop system to the limit of the slugging/non-slugging boundary, similar to what is examined in paper E.

### 2.2.2 Gas-lifting

The external gas lifting in general serves two purposes: (i) For a well: Enabling the mature and depleted reservoirs with low pressure to keep reasonable production rates by injecting gas at the bottom of the well, and (ii) for a riser: Preventing riser-induced slugging by injecting gas at riser base to reduce the hydrostatic pressure and thus also preventing the gas accumulation.

Several control schemes have been suggested for eliminating the slugging with gas-lifting mechanishms [17, 46–48, 95]. Most of the control schemes require boosting the gas injection, which sometimes can be constrained by the capacity of the compressors.

Several alternative well/riser devices have been proposed in combination with gas-lifting control schemes to eliminate the severe slug problems [96, 97], but installation and maintenance are expensive and require hardware changes.

## 2.3 Review of plant-wide offshore automation

Offshore, the oil & gas production is not easily accessible compared to onshore oil & gas production facilities, due to the expensive cost of subsea installations and maintenance, as well as the limited capability for the offshore platforms to satisfy the demands for environmental footprint. The offshore Oil & Gas trends was summarized in [98], where it was concluded that the offshore industry focuses on the development of fields in deeper water, further offshore, with reduced field sizes, which causes further economic challenges due to the reduced revenue available. Thus, the per-barrel cost of recovering hydrocarbons is predicted to increase further in the future [20]. To overcome these economic challenges the amount of subsea equipments is minimized, e.g. by applying multi-phase transportation pipelines instead of several single-phase pipelines [99].

The danish North Sea oil & gas company Mærsk Oil is a partner in this project and have provided some data and information about some current offshore facilities. Like Mærsk Oil, many Oil & Gas operators observe issues with the daily production control and separations processes, which they hope can be more cost-effective with improved process automation. Some of their future ambitions are to:

- Improve the daily production rate by applying intelligent feedback control, as an inexpensive implementation strategy.
- Minimize the cost of separation facilities by improving the automation in installed separation equipment, such as slug catchers, separators and hydrocyclones.
- Investigate available transmitter data. Much data is available, but is not often applied by the operators due to the lack of data and equipment knowledge during changing operating conditions.

A way to archive these ambitions in an effective manner is to operate the process in a *plant-wide* manner, where the subsystems need to coordinate and operate together to optimize the operation [1, 100]. However, this is not well done in the current Oil & Gas installations [21], and thus there is a huge potential in optimizing the operation with plant-wide control. In chapter 2.3.1 the current daily production control will be examined and in chapter 2.3.2 the current separation difficulties are summarized.

### 2.3.1 Actuator manipulation and safety automation

Figure 2 from Paper B, shows an illustration of the gas-lifting mechanism in a production well connected to an oil & gas reservoir. A gas lift valve controls the amount of gas injected from a compressor to the annulus, either by a pressure or flow measurement. A check valve at the well bottomhole guarantees that the gas is injected into the production tubing, where the gas is intended to enhance the production rate. Furthermore, a production valve is installed topside (top of the well) for start-up, shut-down and flow assurance control. The gas-lifting technique is applied in a great part of the production wells worldwide [17,46], but the choice of an optimal gas injection setpoint (controlled by the gas lift valve) is rarely considering the possibility of a flow regime shift from non-slug to severe slug, which can reduce the daily production rate dramatically. The gas-lifting is rarely present in the risers in the North Sea, because the water depths are considered too low to necessitate gas-lifting from a flow assurance perspective. However, there exists several exceptions [97, 101].

In most cases large amounts of injected gas is needed to stabilize the flow [38]. If the required gas injection setpoint does not saturate the compressor it is possible to use the gas-lifting to eliminate the severe slugs. However, it can be a challenge determining this injection setpoint due to the uncertain and varying running conditions [87, 102, 103].

The topside valve is a standard piece of equipment, installed on both wellheads (see the production valve on figure 2) and riser topsides. Sometimes they are originally installed to shut-down, start-up or bypass operations of

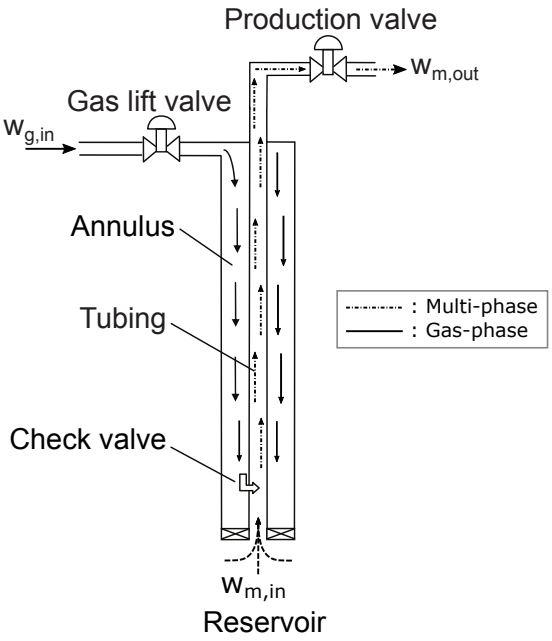


**Fig. 2:** A figure from Paper B, showing the traditional gas-lifting well connected to an oil & gas reservoir.

the individual well or separator, but can also be used to control the flow regimes and production rates. However, many operators try to avoid choking the topside valve, because they know that the decreased valve opening also reduces the production due to the increased induced back pressure [94, 103].

Hence, for both the gas-lifting and valve choking the main objective is to (i) maintain a high production rate (ii) without causing severe slugs, (iii) subject to some operational uncertainties [104]. This can be a challenging task for both a human operator and an automatized control scheme. Figure 3 shows a real topside pressure measurement from an offshore riser located in the North Sea. The pressure transmitter is located topside upstream a choke valve which is connected to a slug catcher linked to a 3-phase separator. In this case there is no gas-lifting installed, and thus the only available solution for changing the flow regime is manipulation of the valve. It is clear that the system is slugging with varying amplitudes and frequencies. However, the topside choke valve is fully open during the entire period, as the operator will not risk a possible production decrease to eliminate the severe slugs, as it is uncertain how much the valve has to be actuated to eliminate the slugs.

During the daily production the topside valve on this North Sea platform is only manipulated for the safety control scheme. The boundaries of the

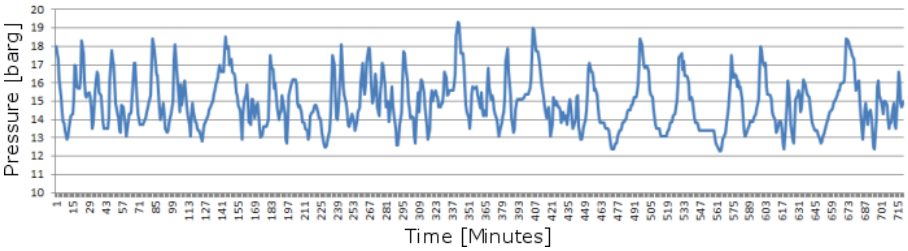


**Fig. 3:** Real data from a separation platform in the North Sea. The time plot shows the topside pressure in barg upstream a 1st stage slug catcher. The topside valve is fully open even thought the flow is clearly slugging with large amplitudes and low frequencies, thus considered severe slug.

| | Capacity * | | Safety alarms | | | |
|---|---|---|---|---|---|---|
| | Maximum | Operation | Low-Low | Low | High | High-High |
| $P_{top}$ $[barg]$ | 220.7 | 15 | 3 | 5 | 28 | 33.3 |
| $h_{s.c.}$ $[m]$ ** | 4.8 | 1-2 | 0.2 | 0.3 | 2.7 | 3.3 |
| $P_{s.c.}$ $[barg]$ ** | 30.3 | 6 | 3 | - | 25 | 27.5 |
| $h_{sep}$ $[m]$ | 3 (Weir plate: 1.52) | 1.3-1.4 | 1 | 1.142 | 1.45 | 2.1 |
| $P_{sep}$ $[barg]$ | - | - | 3.5 | 5 | 23 | 28 |

**Table 1:** The upper and lower safety boundaries causes alarms. The low and high alarms gives a warning to the operator, while the low-low and high-high alarms starts the safety shut-down control procedure.

* The designed operation conditions for optimal production are specified in the Operation entries; the designed maximum safety boundaries are specified in the Maximum entries.

** The slug catcher is denoted s.c. and is physically located downstream the riser and upstream the 3-phase separator to dampen the slugs.

safety alarms are illustrated in table 1, where crossing the low and high alarm thresholds causes notification to the operator and the crossing of the low-low and high-high alarm thresholds causes an automatized shut-down procedure to begin. It is clear that the topside pressure $P_{top}$ in figure 3 stays within the safety region. However, the flow and pressure variations still demand a slug catcher to dampen the severe slugs before the separation process can be efficient. The slug catchers take up a lot of expensive space and require extra maintenance. Thus, one severe consequence of the occurrence of severe slug is the induced issues to the downstream separation process (see chapter 2.3.2).

### 2.3.2 Plant-wide separation difficulties

The produced water is a dominant and increasing problem in the North Sea, as the oil & gas processes produces more and more undesired produced water [105]. The mature wells can get above 90 % water cut [106]. As the water re-injection into the reservoirs is a common cost-effective enhanced recovery approach for the mature oil fields, the tendency is that the water cut will get even bigger in the future [107, 108].

It is forbidden by law to directly discharge the produced water into the ocean. In the North Sea the laws for hydrocarbon discharge are strict; the current limitation of hydrocarbon discharge in the North Sea is 30 $\frac{mg}{l}$ per day [109]. In comparison, the hydrocarbon regulations are maximums of 30 $\frac{mg}{l}$ per day for Australia, 42 $\frac{mg}{l}$ per day for United States Environmental Protection Agency (USEPA) [110] and 40 $\frac{mg}{l}$ per day for countries covered by the OSPAR Convention [105]. Although the existing production installations already struggle to be comply with the current rules, the disposal regulations of hydrocarbon to sea are becoming more and more strict, where the new tendency is zero-discharge of pollutants [111–113].

The high water concentrations require efficient separation equipment to achieve pure oil products. Due to the huge total water volume, more than 40 billion USD is annually dedicated to handling the produced water in the oil & gas sector [114]. Thus, the Produced Water Treatment (PWT) technologies aim for improved separation in a cost-effective manner.

The traditional de-oiling technology in the North Sea consists of 3-phase gravity separators and downstream de-oiling hydrocyclones. This configuration represents 90 % of the existing de-oiling technologies in the North Sea [24, 115]. The first step of the separation consists of a single or multiple 3-phase separators to completely separate the gas and separate most of the oil in the water. This part is physically connected to the topside of the riser on the separation platforms. The water outlet of the last 3-phase separator is connected to a de-oiling hydrocyclone consisting of multiple liners [24, 116]. Figure 4 illustrates the de-oiling separation configuration where the traditional control structures are included.

The typical control structure of both the gravity separator and the hydrocyclone is examined in [24]. The 3-phase separator's water outlet is controlled by a valve dedicated for keeping a constant water height in the separator. The hydrocyclone is often controlled by the pressure drop ratio (PDR), calculated as in equation (1). It indicates how much of the oil-water mixture flow will go through the overflow and underflow, respectively. Ideally all the oil will go to the overflow outlet and all the water to the underflow outlet. The PDR is commonly selected empirically between 1.7 and 2.2 [117–119].

$$PDR = \frac{dP_o}{dP_u} = \frac{P_i - P_o}{P_i - P_u} \tag{1}$$

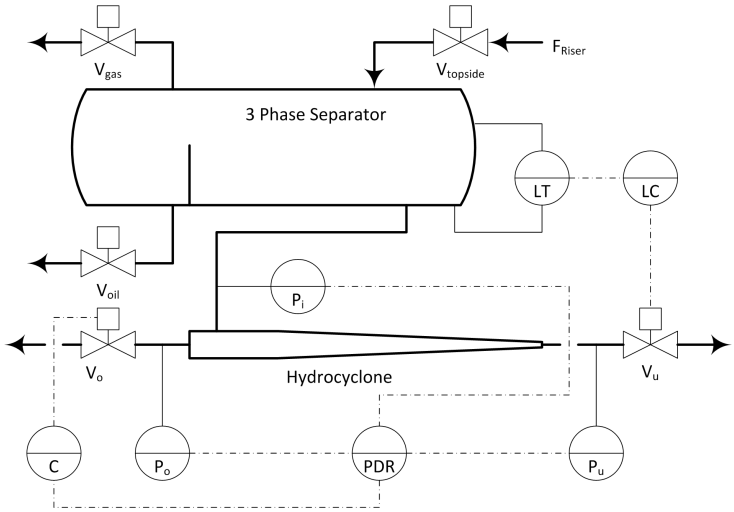


**Fig. 4:** A illustration of the 3-phase gravity separator and de-oiling hydrocyclone configuration for the PWT separation.

A problem occurs if a severe slug flow enters the 3-phase separator. The separator level controller will open the water outlet valve to compensate for the increased multi-phase flow entering the separator druing the liquid blow-out stage, and hence maintain the water level. However, the water outlet will simultaneously experience an increased flow, which impacts the de-oiling hydrocyclone negatively for two reasons: (i) The oil-water mixture entering the hydrocyclone will have a higher oil concentration, which demands a corresponding dynamic adaption of the hydrocyclone separation, and (ii) the varying inflow will affect the hydrocyclone's separation efficiency [24, 120–122]. All in all the existence of severe slugs will clearly result in a long-term reduced separation efficiency if the traditional control structures are applied to the existing separation equipment. The most cost-effective way to avoid this is by either eliminate the severe slugs upstream the separation process, by improving the separation efficiency when severe slug disturbances are present, or by coordinating both actions in a plant-wide control manner.

# 3 Testing rig

Main parts of the work examined in this thesis are based on experiments carried out on a testing facility developed at Aalborg University Esbjerg's laboratory. The facility has continuously been modified and extended throughout the project period and thus three different generations of the test rig have

been applied in the documented work. The construction of the test rig is based on other test rigs documented in [11, 14, 32, 123–128]. The main objective of the test rig is to emulate the severe well- and riser-induced slugs observed on offshore platforms.

The 1st generation rig was operating from august 2013 to may 2014, the 2nd generation rig was operating from september 2014 to june 2015 and the 3rd generation rig have been operating since august 2015. The papers C and E have experimental results from the first generation rig, paper F has results from the 2nd generation rig, and paper G has results from the 3rd generation rig.

## 3.1 1st Generation Testing facility

The first generation test rig was constructed to be economically efficient, and thus the test rig contained a limited number of actuators and transmitters. Figure 5 shows an overview of the constructed test rig, which consists of a inclination pipeline, a riser, a topside section and an open-tank to emulate a 2-phase separator. All transportation pipeline sections were made of transparent PVC, such that the multi-phase flow in all pipelines can be visualized. Water was transported through the pipeline-riser to the separator in a closed flow loop. Air was either injected at the start of the pipeline or riser bottom, transported through the transportation system and let out at the open 2-phase separator tank. A topside choke valve was mounted on top of the riser between two pressure sensors to control the rig's flow regimes. The inclination pipeline could be adjusted from $0^\circ$ to $20^\circ$. The feeding 2-phase inflow consisted of a water pump, which could operate as a pressure or flow source, and a choke valve after an air compressor to control the gas inflow. The air could either be injected at the inlet of the inclination pipeline to emulate the pipeline-riser system or at the riser bottom to emulate the well system. The recreation of riser-induced slugs in the test rig's pipeline-riser section was documented in [58] and the recreation of the casing-heading slugs in the test rig's well section was documented in [47].

The running conditions for the test rig varied depending on the objectives of the respective experiment, but the inlet mass flow rates operated at around $10^{-1}\frac{kg}{s}$ for the liquid (water) phase and $10^{-4}\frac{kg}{s}$ for the gas (air) phase. With these operating conditions the open-loop bifurcation point for the topside choke valve was located at 35%.

## 3.2 2nd Generation Testing facility

From the anti-slug study point of view, the second generation test rig was designed to increase the amplitudes of the slugs, with an increased number of measurements with improved accuracy. This was done by increasing the

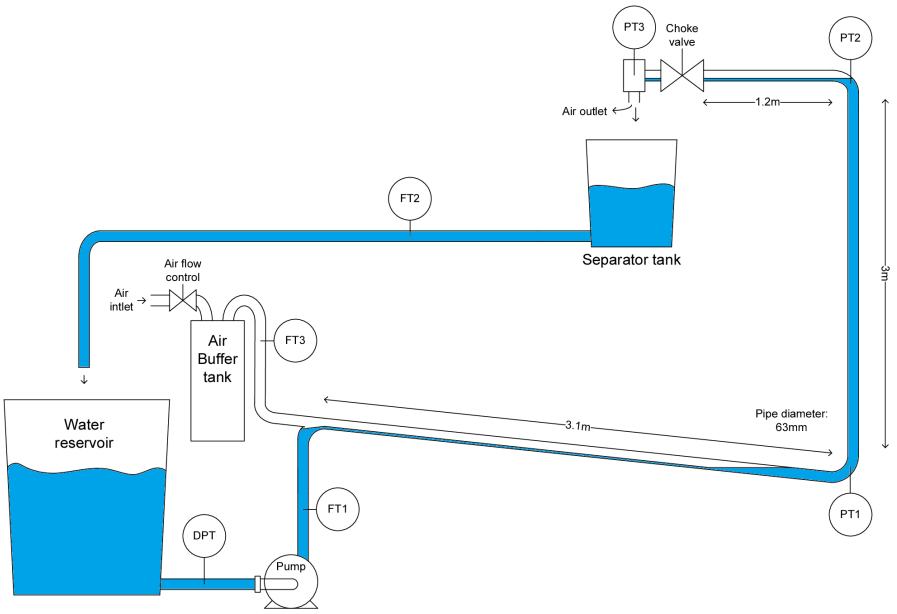


**Fig. 5:** Illustrative drawing of the 1st generation test rig from [58]. The actuators consist of a air flow control valve, a centrifugal pump and a topside choke valve. The transmitters consist of three flow transmitters (FT); two for the inflow and one for the water outflow, three pressure transmitters (PT) and one differential pressure transmitter (DPT) over the pump.

lengths of all pipelines and the amount of transmitters and actuators. The separation processes downstream the well-pipeline-riser system were also included such that the test rig could now operate with the entire system in a compatible manner. Figure 6 shows two 3D-drawings of the second generation test rig: One with the entire setup (figure 6a) and one focusing on the injection, pipeline-riser and separation sections (figure 6b).

The main changes for the second generation test rig are listed here:

- A closed 3-phase separator was added. The system now could be pressurized.
- The riser was extended from 3 to 4.5 meter.
- A 16 meter horizontal pipeline section was added.
- The topside choke valve was changed from a ball valve to a globe valve.
- More transmitters were added.

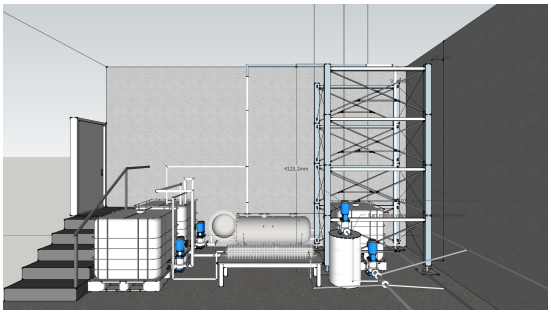

**(a)** The feeding tanks are located to the left and the transportation section to the right.

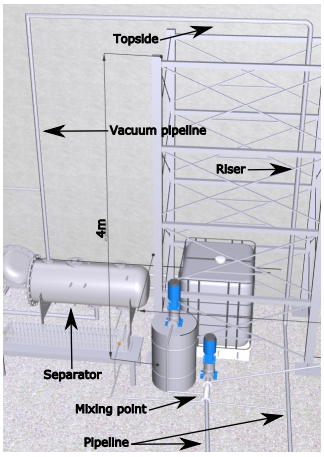


**(b)** Zoomed figure of the inflow and transportation sections.

**Fig. 6:** 3D illustrations of the 2nd generation test rig.

- The gas-lifting now could operate meanwhile the gas inflow was controlled.
- An oil reservoir tank and pump was installed, to be able to run 3-phase (oil/water/air) flow.

The most importation transmitter addition was the Coriolis combined flow and densitometer located topside after the choke valve. The Coriolis transmitter could monitor the slug mass flow variations acceptably, but had increased measurement uncertainties when the gas phase was dominant (eg. during the severe slugs' gas surge stage). The new pressure transmitters had a more targeted and narrow operating range, which heavily improved the signal-to-noise ratio (SNR), which was an issue in the first generation test rig. Furthermore, the test rig could also be pressurized, as a closed 3-phase separator was installed on ground level downstream a vacuum pipeline after the topside section.

On real platforms the 3-phase separators are located on the topside section after the choke valve, but due to the physical and safety restrictions in the laboratory it was not possible to install the separator topside. Hence the purpose of installing the vacuum pipeline was to add an unflooded fall-down section to minimize the cyclically surges as part of the siphon effect [129]. However, the vacuum pipeline still observed some small cyclic surge oscillations, and the vacuum pipeline itself actually detached the transportation and the separation systems, as the vacuum pipeline also acted like a buffer tank prior to the actual separation process. This was a motivation to lift the

separator to topside level in a new laboratory, which was done on the third generation test rig.

## 3.3 3rd Generation Testing facility

The third generation test rig is the current existing test platform still operating at the campus laboratory. The pipeline and riser lengths are now further extended to emulate larger slugs.

The new main additions in the third generation test rig are listed here:

- The gravity separator is now located topside downstream the choke valve to avoid the siphon effect of the vacuum pipeline.
- The vertical riser length has been extended from 4.5 to 6 meters.
- The horizontal pipeline length has been extended from 16 to 30 meters.
- The inclination pipeline length has been extended from 4 to 12 meters.
- More transmitters have been added.

A P&ID drawing is giving an overview of the entire 3rd generation test rig in figure 7. The P&ID diagram illustrates the entire plant-wide test rig, and thus also the equipment extensions in the separation process downstream the pipeline and riser sections.

An extended illustration of the reservoir can be seen on figure 8a. The reservoir section takes care of the inflow supply related equipment including the mixing of the water, oil and gas at the pipeline inlet. The transportation pipeline related equipment can be seen on figure 8b, where the outlet goes into the 3-phase separator. It can also be noted that there exist several pipeline bypassing options to operate with isolated parts of the systems, respectively. It is possible to run each of the following subsystem configurations: A pipeline, a pipeline-riser, a well, one to two separators, one to three hydrocyclones, and any combination of the mentioned separators and hydrocyclones. This gives a huge flexibility as the system can, within 45 seconds (the switch valves' maximum opening/closing time) switch between any of the listed configurations.

## 3.4 Data acquisition

The main operating objective of the test rig is to fulfill the following criteria:

- Operate in MATLAB environment, similar to what is used for the modeling and controller design.
- Apply a normal PC for configuration of the running conditions and running the experiments.

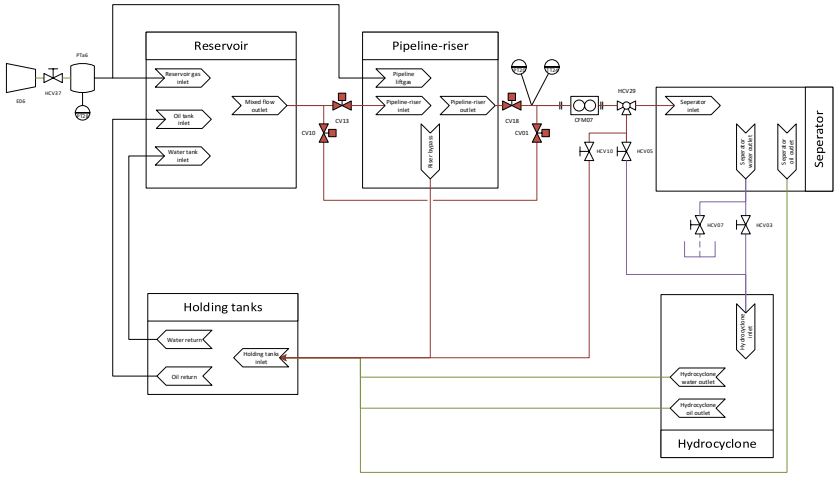


**Fig. 7:** An overview P&ID drawing of the 3rd generation test rig, with the following subparts: Reservoir, pipeline-riser, 3-phase separator, hydrocyclone and lastly a holding tank section for fully separating the oil and water.

- Run real-time with a sampling rate faster than 30 Hz.

All data acquisition and control is performed using a standard host PC running Simulink Real-time (xPC) through a target computer. Four National Instruments (NI) data acquisition and output PCI cards are connected to the target PC. All the sensors and actuators of the system are connected to these four cards using breakout boards and screw terminals. The target PC is dedicated to run data capture and control experiments in real-time. It runs the Simulink real-time target operating system compatible with MATLAB 2014a and later and guarantees real-time simulations, which can be difficult to do otherwise. Models can be uploaded through a direct ethernet connection from the standard PC, and thus the standard PC can be used directly by the operator to design the experiments.

A Simulink component has been developed for the test rig. It is useable to acquire all the sensor signals and convert them to physical units, and is also able to control all actuators. The component represents the entire experimental facility as one block which internally includes one masked block for each DAQ PCI-card measurement interface, and one masked block for each DAQ PCI-card output interface.

The transmitter and actuator signals must be 0-10 V voltage signals with anti-aliasing filtering in order to be captured by the DAQ PCI-cards. Most of the transmitters of the system utilize passive 4-20 mA analogue current

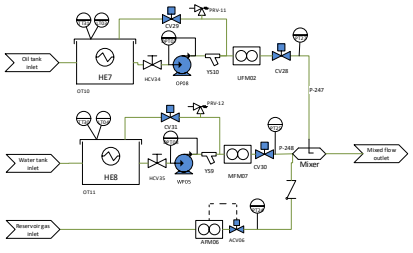


**(a)** A P&ID drawing of the 3rd generation test rig's reservoir section. This section takes care of the inflow to the inlet pipeline.

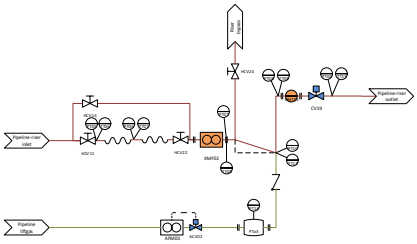


**(b)** An overview P&ID drawing of the 3rd generation test rig's pipeline-riser section which also can operate isolated either as a horizontal pipeline, inclination pipeline-riser or well, depending on the operators configuration.

**Fig. 8:** The 3rd generation test rig's reservoir and pipeline-riser sections, respectively.

signals. These signals are converted to voltage signals using 470 $\Omega$ $\pm$1% resistors connected between the sensor return signals and analogue ground. In addition the filters are using capacitors in parallel, giving first-order low-pass filters with cutoff frequency of approximately 100 Hz, which also eliminates most of the HART digital carrier signal.

In this way the test rig can be manipulated directly from a standard PC in the familiar MATLAB environment with fast sampling rate (100 Hz in this case) guaranteed real-time simulations, while the online measurements can be observed on a monitor screen connected to the target PC.

## 3.5 Inflow controllers

The inflow controllers are designed to control the inflow of gas, water and oil, respectively, as observed in figure 8a. The gas inflow is controlled by a valve after a compressor, and the oil and water phases are each separately controlled by a pump, a valve at a reservoir-feedback pipeline and a valve to the pipeline inlet.

It is clear that there are many possible combinations to emulate the fluid inflow rates to the system, such as emulating flow or pressure sources. It is critical to have fast and reliable inflow controllers to emulate realistic oil & gas production plants. In this thesis' experiments two inflow scenarios are considered: (i) Emulating a flow source for both gas and liquid, and (ii) Emulating a production well by manipulating the liquid pump voltages and regulating the Gas Volume Fraction (GVF) with the gas inflow controller. The GVF is calculated as:

$$GVF = \frac{Q_g}{Q_g + Q_l} \tag{2}$$

where Q is volumic flow measured in $\frac{m^3}{s}$. The gas inflow valve is fast compared to the time constant of the fluid dynamics and with an implemented PID controller the gas inflow can settle down to the given setpoint within a second.

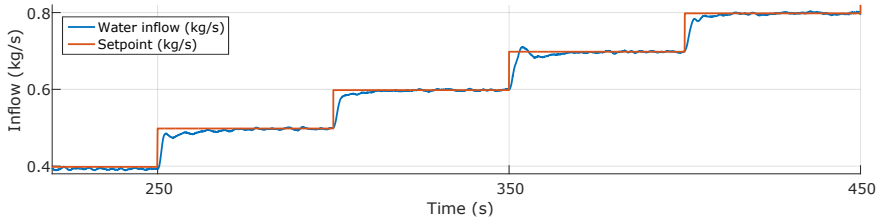


**(a)** A step test with the corresponding step responses of the water mass inflow. The implemented PI controller aims for not overshooting, while keeping a relatively fast settling time with no steady-state error.

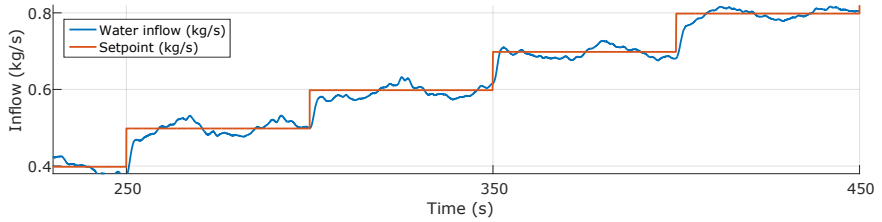


**(b)** A step test with the corresponding step responses of the water mass inflow. The air mass inflow is varying from 0 to 18 $\cdot 10^{-4} \frac{kg}{s}$ as a sinusoidal wave with a 30 seconds cycle time length. Thus, the air inflow causes a large disturbance to the water inflow controller, as the varying air inflow corresponds to varying back pressure in the pipeline.

**Fig. 9:** Step responses for the water mass inflow with and without air inflow disturbance.

The water mass inflow controller is based on a PI control scheme. The controller's objective is to avoid output overshooting while keeping a relatively fast settling time with no steady-state error. An overshoot can cause the flow regime to change, which undesirably affects the transient behavior for the pipeline flow dynamics and can even lead to a misleading flow regime. Figure 9a shows several step responses (0.05 $\frac{kg}{s}$ once every 50 second) for the water mass inflow. The figure clearly shows that the controller tracks the setpoint acceptably as steady-state is settled within a few seconds, while the occasional minor overshooting is insignificant.

When disturbances are added to the system the controller is challenged as it has to track the setpoint while rejecting the varying disturbance. In

Figure 9b a large sinusoidal air inflow is applied to the test rig. The water inflow controller struggles to track the setpoint, with oscillations $\pm 6\%$. This is actually an acceptable result as the GVF vary from 0 to 0.78 within 15 seconds. In the experiments applied in this thesis the GVF will only be slowly changed if not kept constant. For this reason the water inflow controller works acceptable for reliable setpoint tracking.

# 4 Modeling

The modeling examined in this thesis is based on two different independent low-dimensional control-oriented models. The two models are based on two different modeling principles, which both will be described respectively in chapter 4.1 and 4.2. The model extensions developed in this thesis' work will be examined in chapter 4.3.

## 4.1 Di Meglio model

The modeling principles examined in this chapter is based on [75, 76]. The original model was developed in 2009 and further extensions have been made since.

The model concerns a riser. The model introduces a virtual valve at the bottom of the riser which only blocks the inflow gas if and only if the slug occurs. This way the model can simulate the pressure accumulation induced by the inflow gas at riser bottom.

The model consists of 3 differential equations based on mass balance principles. Figure 10 shows the model's geometry which consist of 3 volumes. These are respectively the gas blocked by the virtual valve, the gas in the riser, and the liquid in the riser. The build up of gas induced by the virtual valve causes an increasing pressure which will cause instability.

The 3 differential equation are as follows:

$$\dot{m}_{g,eb} = (1-\epsilon)\omega_{g,in} - \omega_g \tag{3}$$

$$\dot{m}_{g,r} = \epsilon\omega_{g,in} + \omega_g - \omega_{g,out} \tag{4}$$

$$\dot{m}_{l,r} = \omega_{l,in} - \omega_{l,out} \tag{5}$$

$\omega_g$ is the flow through the virtual valve. $\epsilon$ determines the amount of gas directly bypassing the virtual valve. $\omega_{l,in}$ and $\omega_{g,in}$ are the system inflows, and $\omega_{g,out}$ and $\omega_{l,out}$ are the outflows from the choke valve and are defined as the complete mass flow multiplied with the gas-liquid mass ratio in the riser:

$$\omega_{g,out} = \frac{m_{g,r}}{m_{g,r} + m_{l,r}}\omega_{out} \tag{6}$$

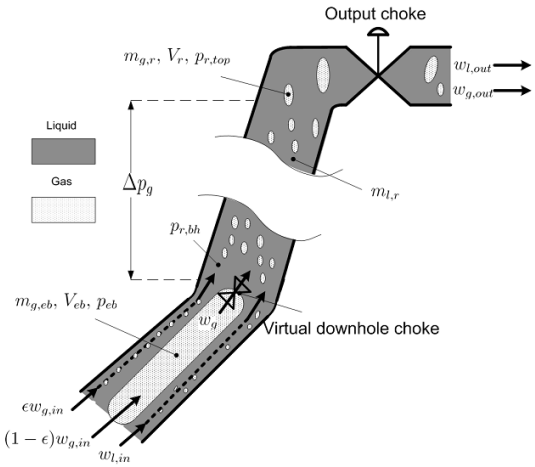


**Fig. 10:** Geometry of the riser model developed by Di Meglio in 2009 [75].

$$\omega_{l,out} = \frac{m_{l,r}}{m_{g,r} + m_{l,r}} \omega_{out} \tag{7}$$

The flow trough the virtual valve and the choke valve are described by linear function of the pressure drop over the valves. It is assumed no backflow is present.

$$\omega_{g,r} = C_g \sqrt{max(P_{eb} - P_{r,bh}, 0)} \tag{8}$$

$$\omega_{out} = z \cdot C_c \sqrt{max(P_{r,top} - P_s, 0)} \tag{9}$$

The different pressures are calculated as follows. First the pressure in the gas bubble generated due to the virtual valve:

$$P_{eb} = \frac{RT}{MV_{eb}} m_{g,eb} \tag{10}$$

where $V_{eb}$ is the volume upstream riser at which the gas can be compressed. The pressure at the top of the riser is:

$$P_{r,top} = \frac{RT}{M(V_r - \frac{(m_{l,r} + m_{still})}{\rho_l})} m_{g,r} \tag{11}$$

and the pressure at the bottom of the riser is:

$$P_{r,bh} = P_{r,top} + \frac{g \sin\theta}{A} \cdot (m_{l,r} + m_{still}) \tag{12}$$

$m_{still}$ is applied as a tuning parameter and indicates the liquid which never leaves the riser during the slug blowout.

It is clear that the model is relatively simple with few equations. The simplicity is the main advantage of the model, as it can easily be understood, applied for model analysis and included in a model-based control scheme. The disadvantage is that the model without any extensions only can be applied for a riser case. Besides, in [71] it was concluded that the model in general was less accurate than other available low-dimensional slug models.

## 4.2 Jahanshahi-Skogestad model

The modeling principles examined in this chapter is based on [44, 71, 77]. The original model was developed in 2011 and further extensions have been made since. The original pipeline-riser model consists of 4 states and the well extension adds 2 extra states; thus the entire well-pipeline-riser model has 6 states. In this chapter the 4 state pipeline-riser model will be examined.

The geometry of the model considers the pipeline and riser as two separate parts. The model consists of 4 states which are based in the mass conservation of liquid and gas in the pipeline and riser section, respectively. Therefore the state equations are as follows:

$$\dot{m}_{G1} = \omega_{G,in} - \omega_{G,lp} \tag{13}$$

$$\dot{m}_{L1} = \omega_{L,in} - \omega_{L,lp} \tag{14}$$

$$\dot{m}_{G2} = \omega_{G,lp} - \omega_{G,out} \tag{15}$$

$$\dot{m}_{L2} = \omega_{L,lp} - \omega_{L,out} \tag{16}$$

Where $\omega_{L,lp}$ and $\omega_{G,lp}$ is the mass flow of liquid and gas from the pipeline to the riser section. These flows can be described by a virtual valve equation.

**Flow at low point:**

The mass flow of gas is blocked when the bottom of the riser is filled with liquid and the flow will be zero. This is illustrated in figure 11b

$$\omega_{G,lp} = 0, \ for \ h_1 \geq h_c \tag{17}$$

And when it is not blocked as in figure 11a the flow is described as:

$$\omega_{G,lp} = K_G A_G \sqrt{\rho_{G1} \Delta P_G}, \ for \ h_1 < h_c \tag{18}$$

where the pressure over the low point is:

$$\Delta P_G = P_1 - \Delta P_{fp} - P_2 - \overline{\rho}_m g L_2 - \Delta P_{fr} \tag{19}$$

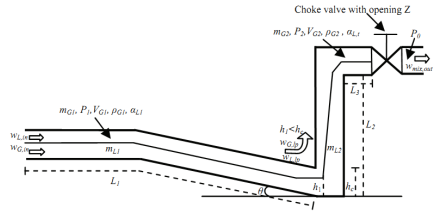


**(a)** Geometry of pipeline and riser when low point is unblocked.

**(b)** Geometry of pipeline and riser when low point is blocked.

**Fig. 11:** The switching mechanism of the Jahanshahi-Skogestad model [71].

and the area of the opening is:

$$A_G = \pi r_1^2 \left( \frac{h_c - h_1}{h_c} \right), \; for \; h_1 < h_c \tag{20}$$

$h_1$ is the height of the liquid in the bottom of the riser. $h_c$ is the height to be filled before the bottom of the riser is blocked.

$$h_1 = K_h h_c \overline{\alpha}_{L1} + \left( \frac{m_{L1} - \rho_L V_1 \overline{\alpha}_{L1}}{\pi r_1^2 (1 - \overline{\alpha}_{L1}) \rho_L} \right) \sin\theta \tag{21}$$

The liquid mass flow is also described by a orifice equation:

$$\omega_{L,lp} = K_L A_L \sqrt{\rho_L \Delta P_L} \tag{22}$$

And the pressure over the low point is:

$$\Delta P_L = P_1 - \Delta P_{fp} + \rho_L g h_1 - P_2 - \overline{\rho}_m g L_2 - \Delta P_{fr} \tag{23}$$

Where the area of the opening is depending on the area of gas mass flow:

$$A_L = \pi r_1^2 - A_G \tag{24}$$

**Inflow conditions:**

The average liquid fraction in the pipeline can be approximated by the following:

$$\overline{\alpha}_{L1} \cong \frac{\overline{\rho}_{G1} \omega_{L.in}}{\overline{\rho}_{G1} \omega_{L.in} + \rho_L \omega_{G.in}} \tag{25}$$

where the gas density can be calculated based on nominal pressure of the pipeline:

$$\rho_{G1} = \frac{P_{1,nom} M_G}{R T_1} \tag{26}$$

**Pipeline equations:**
Volume of pipeline section:

$$V_1 = \pi r_1^2 L_1 \tag{27}$$

Volume of riser pipeline filled with gas:

$$V_{G1} = V_1 - \frac{m_{L1}}{\rho_L} \tag{28}$$

Density of gas in pipeline section:

$$\rho_{G1} = \frac{m_{G1}}{V_{G1}} \tag{29}$$

Pressure in pipeline section:

$$P_1 = \frac{\rho_{G1} R T_1}{M_G} \tag{30}$$

Pressure lost due to friction in pipeline:

$$\Delta P_{fp} = \frac{\overline{\alpha}_{L1} \lambda_p \rho_L \overline{U}_{sl,in}^2 (L_1)}{4 r_2} \tag{31}$$

With friction faction:

$$\lambda_p = 0.0056 + 0.5 Re_p^{-0.32} \tag{32}$$

and Reynolds number:

$$Re_p = \frac{2 \overline{\rho}_L \overline{U}_{sl,in} r_1}{\mu} \tag{33}$$

and superficial velocity of the liquid:

$$\overline{U}_{sl,in} = \frac{\omega_{L,in}}{\rho_L \pi r_1^2} \tag{34}$$

**Riser equations:**
Volume of riser section:

$$V_2 = \pi r_2^2 (L_2 + L_3) \tag{35}$$

Volume of gas in riser section:

$$V_{G2} = V_2 - \frac{m_{L2}}{\rho_L} \tag{36}$$

Density of gas in riser section:

$$\rho_{G2} = \frac{m_{G2}}{V_{G2}} \tag{37}$$

Pressure in riser section:

$$P_2 = \frac{\rho_{G2} R T_2}{M_G} \tag{38}$$

The average liquid fraction in the riser:

$$\overline{\alpha}_{L2} = \frac{m_{L2}}{V_2 \rho_L} \tag{39}$$

mixture density in riser section:

$$\overline{\rho}_m = \frac{m_{G2} + m_{L2}}{V_2} \tag{40}$$

Pressure lost due to friction in riser:

$$\Delta P_{fr} = \frac{\overline{\alpha}_{L2} \lambda_r \overline{\rho}_m \overline{U}_m^2 (L_2 + L_3)}{4 r_2} \tag{41}$$

With friction faction:

$$\lambda_r = 0.0056 + 0.5 Re_r^{-0.32} \tag{42}$$

and Reynolds number:

$$Re_r = \frac{2 \overline{\rho}_m \overline{U}_m r_2}{\mu} \tag{43}$$

Average mixer velocity in riser:

$$\overline{U}_m = \overline{U}_{sl2} + \overline{U}_{sg2} \tag{44}$$

$$\overline{U}_{sl2} = \frac{\omega_{L,in}}{\rho_L \pi r_2^2} \tag{45}$$

$$\overline{U}_{sg2} = \frac{\omega_{G,in}}{\rho_{G2} \pi r_2^2} \tag{46}$$

**Outflow conditions:**
The output flow is calculated using a orifice equation:

$$\omega_{mix,out} = K_{pc} f(z) \sqrt{\rho_t (P_0 - P_2)} \tag{47}$$

where $\rho_t$ is the mixed density at the top of the riser. $P_0$ is the pressure after the choke valve. $f(z)$ is the valve function which is assumed linear. $K_{pc}$ is a tuning variable. The liquid output flow is found as:

$$\omega_{L,out} = \alpha_{Lm,t}\omega_{mix,out} \tag{48}$$

And the gas output flow:

$$\omega_{G,out} = (1 - \alpha_{Lm,t})\omega_{mix,out} \tag{49}$$

$\alpha_{Lm,t}$ is the liquid fraction at the top of the riser and can be calculated as follows:

$$\alpha_{Lm,t} = \frac{\alpha_{L,t}\rho_L}{\alpha_{L,t}\rho_L + (1 - \alpha_{L,t})\rho_{G2}} \tag{50}$$

The liquid fraction in the riser can by approximated to be the average of the faction at the bottom and the top of the riser as follows:

$$\alpha_{L,2} = \frac{\alpha_{L,lp} + \alpha_{L,t}}{2} \tag{51}$$

The liquid fraction at the bottom of the riser can be calculated as:

$$\alpha_{L,lp} = \frac{A_L}{\pi R_1^2} \tag{52}$$

and therefore the liquid faction at the top of the riser can be calculated as:

$$\alpha_{L,t} = 2\overline{\alpha}_{L2} - \alpha_{L,lp} \tag{53}$$

The Jahanshahi-Skogestad model is slightly more complicated than the Di Meglio model. Contrary to the Di Meglio model, this model does not only include a vertical pipeline, but also the entire pipeline-riser (or the well-pipeline-riser). This addition can be useful for a plant-wide system consideration. Besides, the Jahanshahi-Skogestad model has the potentially to be more accurate than the Di Meglio model [71]. The many tuning parameters of the Jahanshahi-Skogestad model also makes it much harder to tune than the simpler models.

## 4.3 Model comparison and modifications

The model tuning was weighted with the following prioritized order of model-to-data precision for the model outputs:

1. Open-loop bifurcation point.
2. Non-slug stable steady-state value.
3. Transient behavior (based on step responses).
4. Slug average steady-state value.

5. Maximum and minimum slug peaks.

Especially bullet point 1-3 was weighted significantly dominant in the tuning process. It also has to be noted that it is difficult to make a good fit for all 5 bullet points, due to the relative simple physics in the low-dimensional models considered. To improve the accuracy, the models were extended with some modifications.

When more accuracy was needed the Di Meglio model was replaced with the Jahanshahi-Skogestad model, as previous literature have concluded that this model is potentially more accurate [44, 71, 77]. This model change improved the accuracy of the model's flow outputs. Furthermore several model modifications have been carried out for the models, mainly for the Jahanshahi-Skogestad model to further improve the accuracy. The main modifications will be listed in subchapter 4.3.1, 4.3.2 and 4.3.3. Only the ball valve characteristics in chapter 4.3.1 is applied to the Di Meglio model, where the rest is modifications to the Jahanshahi-Skogestad model.

### 4.3.1 Static valve opening characteristics

In most choke valves' data sheets the flow coefficient ($C_v$) can be obtained, but this normally only applies for single phase liquids and not multi-phase fluids. In this chapter the opening characteristics will be examined instead, as this can be used to determine the function, $f(z)$. The valve static opening characteristics have been modified from the original linear form where

$$f(z) = z \; for \; 0 \leq z \leq 1 \tag{54}$$

which fits plug-and-cage valves. The first generation test rig applied a topside ball valve, which was later modified in the second and third generation to a topside globe valve, as globe valves are the preferred control valves in the offshore oil & gas installations. The ball valves opening characteristics is based on the sigmoid function

$$f(z) = \frac{1}{1 + e^{-a_1(z-b_1)}} \; for \; 0 \leq z \leq 1 \tag{55}$$

where $a_1 = 8$ and $b_1 = 0.6$ for the topside ball valve on the first generation test rig. A ball valve is normally used for open/closed operations. One of the advantages of ball valves is that the flow orifice in open position equals the entire pipe cross section size, and thus induces no back pressure or the corresponding production reduction.

The fast opening globe valve's characteristic equation is

$$f(z) = a_2 \cdot e^{b_2 \cdot z} \; for \; 0 \leq z \leq 1 \tag{56}$$

where $a_2 = 0.05$ and $b_2 = 3$ for the topside globe valve on the second generation test rig. For continuous valve operations globe valves are a good choice. The biggest limitation of using the globe valve is the relatively large pressure drop over the valve even when fully open.

The inclusion of the valve characteristics improved the accuracy for both models. Without this extension the model (with the linear valve characteristics) could only be accurate to the data in a small valve opening region, whereas the updated models now could fit most of the opening region, such that the model is assumed to be very accurate in the entire operatinal region ($5\% \geq z \geq 100\%$). To improve the accuracy for the low valve openings outside the operational valve region, extended valve characteristics have to be considered.

### 4.3.2 Darcy friction factor

Darcy frictions are commonly applied to estimate the friction loss in the process. The Darcy friction factor is estimated based on the Reynold number for the given pipeline section. There exist several equations for estimating the Darcy friction factors for pipeline. For the horizontal and inclination pipeline equation (32) is applied and for the riser equation (57) is applied.

$$\frac{1}{\sqrt{\lambda_{riser}}} = -1.8 \cdot log_{10}\left(\left(\frac{\epsilon}{D_r \cdot 3.7}\right)^{1.11} + \frac{6.9}{Re_r}\right) \tag{57}$$

Furthermore, in the original Jahanshahi-Skogestad model no friction loss is considered for the topside horizontal pipeline section ($L_3$). This friction loss is added in this thesis' work. The pressure upstream the topside (globe) choke valve ($P_{t,v}$) is derived from the topside pressure ($P_t$) added to the pressure generated by the topside pipeline friction ($P_{t,f}$), such that

$$P_{t,v} = P_t - P_{t,f} \tag{58}$$

The topside valve equation now uses $P_{t,v}$ instead $P_t$. The value of $P_{t,v}$ will vary further from $P_t$ the longer the topside choke valve is located from the riser top. The friction for $P_{t,f}$ is calculated similarly to the riser friction in equation (57).

The modifications in the pipeline friction loss improves the accuracy of the model's ability to estimate the pressure outputs precisely.

### 4.3.3 Added tuning parameter

Besides the added static tuning parameters added in the valve characteristic equations, a new tuning parameter ($K_a$) is added for the Jahanshahi-Skogestad model, see equation (59). $K_a$ operates similar to the $m_{still}$ tuning parameter in the Di Meglio model, and intends to correct for how much of

the liquid is flowing through the riser during the blowout stage of each slug cycle.

$$\alpha_{L,rt}(t) = K_a(2\alpha_{L,r}(t) - \alpha_{L,rb}(t)) = K_a\left(\frac{2m_{l,r}(t)}{V_r\rho_L} - \frac{A_{L,rb}(t)}{A_{p,rb}}\right) \tag{59}$$

where

$$1 \geq \alpha_{L,r} \geq \alpha_{L,rt} \geq 0 \tag{60}$$

With the addition of the new tuning parameter, the model's pressure offset in the riser can be adjusted very accurately down to below one percentage variation from the obtained test data.

# 5 System analysis

This chapter will examine the properties of the flow regime and bifurcation mapping strategies in chapter 5.1 which is investigated in Paper A, B, and C, and the Input-Output (IO) controllability model analysis in chapter 5.2 which is investigated in Paper F.

## 5.1 Flow and bifurcation mapping

The traditional methods for understanding the occurrence of severe slugs are based on flow maps and bifurcation maps [9, 130, 131]. These methods are commonly used by process engineers and operators in the oil & gas industry. The creation of the maps requires lots of experimental data [132–134], although several studies have focused on estimating slug criteria based on mathematical approaches, to avoid severe slugs already in the design stage [38, 123, 133, 135–143]. However, the experimental maps can still be an indicator of how severe the slugs are, how frequently they occur and how much control effort is required for eliminating them.

The flow maps show which flow regime is present during steady-state for specific liquids and gases superficial velocities. The superficial velocity ($v_{sup}$) is defined as:

$$\frac{\omega}{\rho A_{cross}} = v_{sup} \tag{61}$$

where $A_{cross}$ is the cross area section over the pipeline. Figure 12 shows the flow map for the 3rd generation test rig, where the two colors indicate the slug (blue) and non-slug (red) regions, respectively. Riser-induced slug flow is generally present at the low gas and liquid flow ranges, which also has been concluded in previous literature [133, 135]. Figure 12 is focused on the

lower non-slug/slug boundaries of the flow map, however if the flow ranges were increased the higher boundaries would be observable as well. Thus, the entire flow map's lower and higher boundaries indicate that the test rig can emulate the riser-induced slugs accurately.

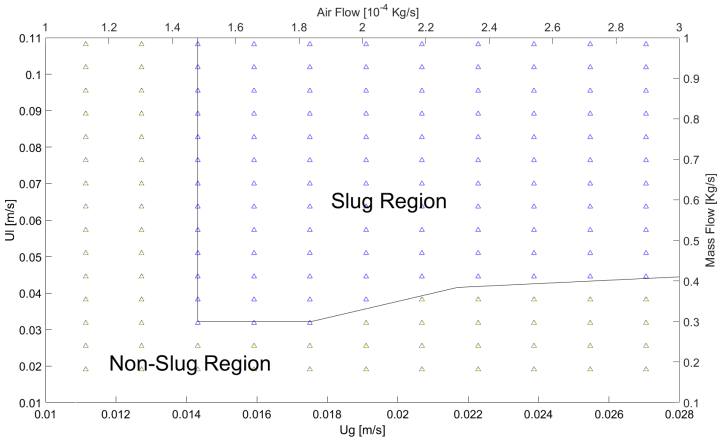


**Fig. 12:** A flow map from the 3rd generation test rig with respect to the superficial velocity of gas and liquid, respectively. Blue is slug flow region, and yellow is the non-slug flow region.

The bifurcation map is normally obtained when the running conditions are constant and only the topside choke valve is manipulated. Then the output parameters (normally pressures or mass flow rates) are plotted with respect to the valve opening. Figure 13 from Paper B shows a general Hopf Bifurcation map, plotting the riser base pressure, where the Bifurcation point indicates the boundary between the slug and non-slug flow regimes. It has to be noted that the bifurcation points only indicate the steady-state output peaks and average output values for fixed valve openings and are thus not considering varying valve openings.

In Paper C it was observed that the Flow and Bifurcation maps influence each other, such that a new operating condition in the flow map will effect the bifurcation map as well. A new 3D-map is developed, which combines the information from both traditional plots into one mapping. Here the considered output is mapped with color to visualize the effect of changing the process' running conditions. Figure 14 shows one of the maps developed in Paper C. The map shows the stable surface for the three independent parameters: Superficial gas, superficial liquid and topside valve opening. It is clear that the bifucation point increases for high liquid and gas flow rates. This new plot can help operators navigate towards a stable region at which the pressure is low and the gas and liquid inflows are within the feasible region. Furthermore, with some minor modification the new-proposed 3D map can

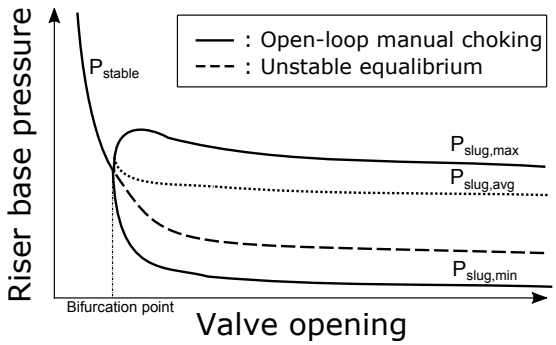


**Fig. 13:** A general schematic showing a Hopf Bifurcation from Paper B. The Bifurcation point is indicating the boundary between the slug and non-slug flow regimes.

also work for closed-loop scenarios with controlled parameters, such as superficial gas inflow and topside choking. In that case the stable surface will indicate the closed-loop stable boundaries, in a similar way as figure 14 illustrates the open-loop stable surface. More details of the new-developed map can be found in Paper C.

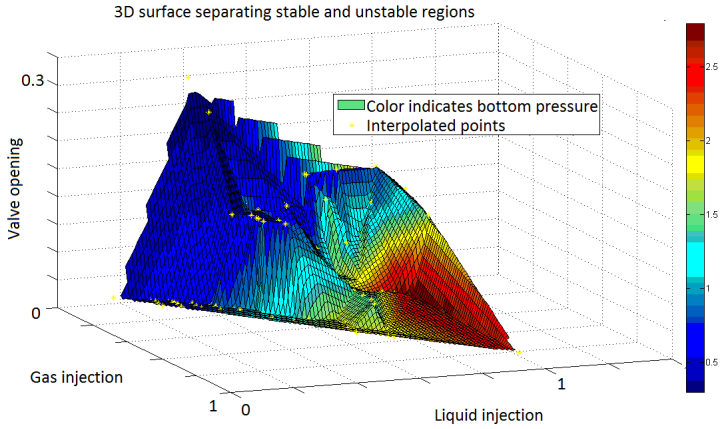


**Fig. 14:** Modified figure from Paper C. The new-developed 3D map with color indicating the bottom pressure output ($P_b$). The data is obtained from the 1st generation test rig.

## 5.2 IO controllability analysis

The model analysis in this thesis is mainly based on the Input-output (IO) controllability analysis on the individual linearzied transfer functions for

each in- and output, respectively. Hence, the IO controllability examined in this chapter is based on the Jacobian linearizations of the nonlinear Jahanshahi-Skogestad slug model. The methods examined in this chapter is based on theory from [50, 78, 144] and is documented in details in Paper F. Furthermore, the results from table 2, 3, 4, and 5 are also from Paper F with minor modifications. The IO controllability is defined in definition 1 quoted from [145].

**Definition 1.** *(Input-output) Controllability is the ability to achieve acceptable control performance, that is, to keep the outputs (y) within specified bounds or displacements from their setpoints (r), in spite of unknown variations such as disturbances (d) and plant changes, using available inputs (u) and available measurements (e.g. $Y_m$ or $d_{in}$).*

The applied the IO controllability analysis in this thesis is carried out similarly to previous slugs studies, such as [43, 50, 78], where the model's IO controllability properties are estimated by finding the minimum achievable maximum peak values in the frequency domain (the lower bounds of the $H_\infty$ norm) of various transfer function's of the linearized model. The peaks are found by obtaining the maximum value of the frequency magnitude response known as the system's $H_\infty$ norm,

$$||M||_\infty = \max_{0 \leq \omega \leq \infty} ||M(j\omega)|| \,. \tag{62}$$

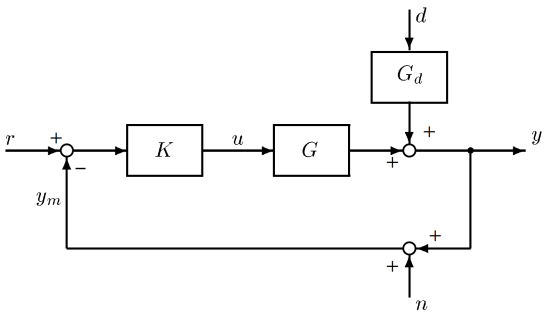


**Fig. 15:** Block diagram showing the considered system including output disturbance (d) and measurement noise (n).

Consider a linearized model where the output is $y = G(s)u + G_d(s)d$ with a linear feedback controller $u = K(s)(r - y - n)$. Here d is the disturbances, n is the measurement noise and r is the reference setpoint. The system can be observed on figure 15 where the closed-loop system is illustrated as a block diagram. Thus, the closed-loop system is

$$y = Tr + SG_d d - Tn \tag{63}$$

where S is the sensitivity transfer function, such that $S = (I + GK)^{-1}$, and T is the complementary sensitivity transfer, such that $T = GK(I + GK)^{-1}$. The control input to the closed-loop system is

$$u = KS(r - G_d d - n) \tag{64}$$

.

For the considered configuration $SG$, $KS$, $SG$, $S$ and $T$ related to the robustness of different types of uncertainties and disturbances. It is preferred to keep their $H_\infty$ norms as small as possible to improve system robustness [50].

## 5.3 Lower bounds

The lowest achievable peaks' boundaries for the considered linearized model in this chapter, is estimated based on the equations obtained from [144].

The lowest achievable peak values for $S$ and $T$ are calculated based on the distance between the unstable poles ($p_i$) and zero ($z$) of the open-loop system:

$$\min_K ||S||_\infty \geq M_{S,min} = \prod_{i=1}^{N_p} \frac{z + p_i}{z - p_i} \tag{65}$$

In [146] it was proved that equation (65) also can be applied for the lowest peak boundary calculation of any $T$ with no time delay, i.e. $M_{T,min}$. Furthermore, in [146] a more general boundary calculation was presented for MIMO systems with no time delay which also can handle multiple RHP zeros:

$$M_{S,min} = M_{T,min} = \sqrt{1 + \bar{\sigma}^2(Q_p^{-1/2} Q_{zp} Q_z^{-1/2})} \tag{66}$$

where

$$[Q_z]_{ij} = \frac{y_{z,i}^H y_{z,j}}{z_i + \bar{z}_j},\ [Q_p]_{ij} = \frac{y_{p,i}^H y_{p,j}}{\bar{p}_i + p_j},\ [Q_{zp}]_{ij} = \frac{y_{z,i}^H y_{p,j}}{z_i - p_j}. \tag{67}$$

The transfer function $KS$ describes the relationship between $n$ to $u$, and thus considers the effect of the measurement noise and output disturbances. The lowest peak boundary of $KS$ is estimated according to

$$||KS||_\infty \geq |G_s(p)^{-1}|, \tag{68}$$

where $G_s$ is a stable transfer function where the RHP-poles of $G$ is mirrored into the LHP. When there are multiple and complex unstable poles the peak can be calculated as

$$||KS||_\infty \geq \frac{1}{\underline{\sigma}_H}(U(G)^*), \tag{69}$$

where $\underline{\sigma}_H$ is the smallest Hankel singular value and $U(G)^*$ is the mirrored image of the antistable part of G.

Where $SG$ relates to the input disturbances and robustness against pole uncertainty, $SG_d$ is related to the effect of output disturbances. For any single unstable zero, the lower peak boundaries of the $H_\infty$ norms of two transfer functions for $SG$ and $SG_d$ can be estimated according to equation (70) and (71):

$$||SG||_\infty \geq |G_{ms}(z)| \prod_{i=1}^{N_p} \frac{z+p_i}{z-p_i} \tag{70}$$

$$||SG_d||_\infty \geq |G_{ms,d}(z)| \prod_{i=1}^{N_p} \frac{z+p_i}{z-p_i} \tag{71}$$

where $G_{ms}$ and $G_{ms,d}$ are the minimum phase stable versions of $G$ and $G_d$ as both RHP poles and zeros are mirrored into LHP.

Similarly, the lower boundary of $KSG_d$ can be obtained from

$$||KSG_d||_\infty \geq \frac{1}{\underline{\sigma}_H}(U(G_{d,ms}^{-1}G)^*) \tag{72}$$

where $U(G_{d,ms}^{-1}G)^*$ is the mirror image of the antistable part of $G_{d,ms}^{-1}G$ [50].

The pole vector of each model is obtained for optimal output selection. A large pole vector element suggests the minimum input effort required for stabilization. Equation (73) is applied to calculate the pole vector based on the state-space expression's C (output) matrix. Here $t$ is the right normalized eigenvector associated with the unstable RHP pole ($p$) such that $At = pt$.

$$y_p = Ct \tag{73}$$

Table 2, 3, 4, and 5 from Paper F show the IO controllability results for the model of the 2nd generation test rig with several considered outputs and valve opening linearization points, respectively. The lower bounded peaks are quantified, and can thus compare the different outputs at different operational openings. The quantification can be used to get an idea of the outputs' performance in a SISO control scheme, but it is hard to conclude exactly how a controlled variable will perform in a control scheme as it is only a boundary. Nevertheless it is clear that the topside pressure, $P_t$, is the worst of the considered outputs, as the peaks are high already at low valve openings. The topside flow transmitter, $\omega_o$, seems to be a good topside measurement alternative, and the pipeline inlet pressure, $P_{in}$, and the riser bottom pressure, $P_b$, both perform equally well. Thus, all but $P_t$ seem to be good for SISO control strategies, respectively.

This IO controllability conclusion is later also observed on closed-loop MATLAB and OLGA simulations, where $P_t$ also is found to be the worst of

the considered outputs for all the examined SISO anti-slug control strategies, see table 6. All the results can be found in Paper F.

| Measurement | Equilibrium | G(0) | Pole vector | $\|\|S\|\|_{\infty,min}$ | $\|\|KS\|\|_{\infty,min}$ | $\|\|SG\|\|_{\infty,min}$ | $\|\|KSG_{d1}\|\|_{\infty,min}$ | $\|\|KSG_{d2}\|\|_{\infty,min}$ | $\|\|SG_{d1}\|\|_{\infty,min}$ | $\|\|SG_{d2}\|\|_{\infty,min}$ |
|---|---|---|---|---|---|---|---|---|---|---|
| $P_{in}$ [bar] | 0.36 | -2.62 | 3.67 | 1.00 | 0.05 | 0.00 | 0.17 | 0.32 | 0.00 | 0.00 |
| $P_b$ [bar] | 0.35 | -2.62 | 3.73 | 1.00 | 0.05 | 0.00 | 0.17 | 0.32 | 0.00 | 0.00 |
| $P_t$ [bar] | 0.04 | -2.46 | 1.05 | 1.17 | 0.16 | 1.42 | 0.16 | 0.34 | 0.23 | 0.53 |
| $\omega_o$ [kg/s] | 0.18 | 0.00 | 156 | 1.00 | 0.00 | 0.00 | 0.16 | 0.34 | 0.03 | 32.4 |

**Table 2:** Model analysis for Z = 30 %

| Measurement | Equilibrium | G(0) | Pole vector | $\|\|S\|\|_{\infty,min}$ | $\|\|KS\|\|_{\infty,min}$ | $\|\|SG\|\|_{\infty,min}$ | $\|\|KSG_{d1}\|\|_{\infty,min}$ | $\|\|KSG_{d2}\|\|_{\infty,min}$ | $\|\|SG_{d1}\|\|_{\infty,min}$ | $\|\|SG_{d2}\|\|_{\infty,min}$ |
|---|---|---|---|---|---|---|---|---|---|---|
| $P_{in}$ [bar] | 0.36 | -1.17 | 3.60 | 1.00 | 0.21 | 0.00 | 0.35 | 0.62 | 0.00 | 0.00 |
| $P_b$ [bar] | 0.34 | -1.17 | 3.73 | 1.00 | 0.20 | 0.00 | 0.33 | 0.64 | 0.00 | 0.00 |
| $P_t$ [bar] | 0.03 | -1.10 | 0.58 | 1.88 | 1.31 | 1.44 | 0.32 | 0.68 | 0.23 | 0.53 |
| $\omega_o$ [kg/s] | 0.18 | 0.00 | 192 | 1.00 | 0.00 | 0.00 | 0.32 | 0.70 | 0.03 | 32.4 |

**Table 3:** Model analysis for Z = 45 %

| Measurement | Equilibrium | G(0) | Pole vector | $\|\|S\|\|_{\infty,min}$ | $\|\|KS\|\|_{\infty,min}$ | $\|\|SG\|\|_{\infty,min}$ | $\|\|KSG_{d1}\|\|_{\infty,min}$ | $\|\|KSG_{d2}\|\|_{\infty,min}$ | $\|\|SG_{d1}\|\|_{\infty,min}$ | $\|\|SG_{d2}\|\|_{\infty,min}$ |
|---|---|---|---|---|---|---|---|---|---|---|
| $P_{in}$ [bar] | 0.35 | -0.44 | 3.58 | 1.00 | 0.69 | 0.00 | 0.89 | 1.57 | 0.00 | 0.00 |
| $P_b$ [bar] | 0.34 | -0.44 | 3.76 | 1.00 | 0.65 | 0.00 | 0.84 | 1.60 | 0.00 | 0.00 |
| $P_t$ [bar] | 0.03 | -0.41 | 0.36 | 3.09 | 6.83 | 0.97 | 0.79 | 1.76 | 0.23 | 0.53 |
| $\omega_o$ [kg/s] | 0.18 | 0.00 | 212 | 1.00 | 0.01 | 0.00 | 0.80 | 1.78 | 0.03 | 32.4 |

**Table 4:** Model analysis for Z = 60 %

| Measurement | Equilibrium | G(0) | Pole vector | $\|\|S\|\|_{\infty,min}$ | $\|\|KS\|\|_{\infty,min}$ | $\|\|SG\|\|_{\infty,min}$ | $\|\|KSG_{d1}\|\|_{\infty,min}$ | $\|\|KSG_{d2}\|\|_{\infty,min}$ | $\|\|SG_{d1}\|\|_{\infty,min}$ | $\|\|SG_{d2}\|\|_{\infty,min}$ |
|---|---|---|---|---|---|---|---|---|---|---|
| $P_{in}$ [bar] | 0.35 | -0.14 | 3.57 | 1.00 | 2.35 | 0.00 | 2.73 | 4.79 | 0.00 | 0.00 |
| $P_b$ [bar] | 0.34 | -0.14 | 3.78 | 1.00 | 2.22 | 0.00 | 2.53 | 4.85 | 0.00 | 0.00 |
| $P_t$ [bar] | 0.03 | -0.13 | 0.24 | 4.74 | 34.6 | 0.48 | 2.40 | 5.41 | 0.23 | 0.53 |
| $\omega_o$ [kg/s] | 0.18 | 0.00 | 223 | 1.00 | 0.04 | 0.00 | 2.42 | 5.47 | 0.03 | 32.4 |

**Table 5:** Model analysis for Z = 75 %

# 6 Anti-slug control development and results

Several control strategies have been applied in the examined work. In this chapter a brief explanation of each individual controller will be examined, respectively. Furthermore, the simulation and experimental results using the controllers will also be presented.

## 6.1 Supervisory control

The work carried out in Paper E examines a supervisory anti-slug control strategy with a self-learning reference and switching control scheme, for $P_b$ as measured output and topside choke valve opening ($z$) as input. Figure 16 from Paper E shows the considered control structure where the supervisory controller's learning algorithm updates the reference in an adaptive manner. The supervisor detects the slug based on the output measurement ($P_b$), and based on the detection decision the reference generator finds the optimal closed-loop operating reference point. The selector switches between a set of two PID controllers each with independent objectives: (i) Operating in the slug region with the objective to eliminate the slug, and (ii) operating in the non-slug region for optimizing the production rate.

The main contribution in Paper E is the control strategy involving the self-learning reference generator and a switching control scheme, each with

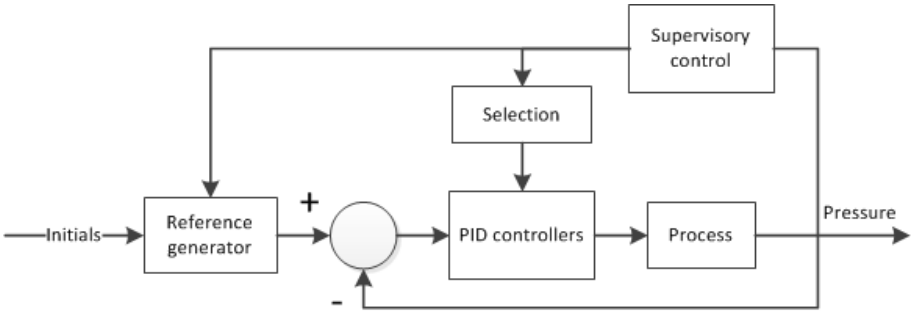


**Fig. 16:** Figure from Paper E illustrating the supervisory control structure for eliminating the slug while finding the optimal operating point with a self-learning reference procedure based on the observed measurements.

different objectives. The experimental results show great improvement in the production rate by implementing the proposed control strategy. This can be observed in figure 17 where the mass flow is plotted with respect to time. The blue line is the mass flow rate and the red line is the average mass flow rate over four slug cycles period of time for comparing the production rate before and after the enabling of the controller. Here, the steady-state production rate is increased by 7.8% in average by applying the proposed supervisory control strategy compared with the initial fully open choke valve (and slugging) scenario.

The main limitation of the control strategy is the long learning procedure which contributes to sensitivity to process and operating condition changes. The learning period is linked to the detection time of the supervisor, and thus a faster supervisor will simultaneously give a faster settling time of the entire closed-loop system. This is proved in Paper E, where the settling time is reduced from 2500 to 300 seconds by adding a correct initial reference point and hence avoiding the self-learning period. However, the steady-state production rate is the same for both cases. Furthermore, the switching control strategy is not restricted to PID controllers only, and thus an improved set of switching controllers which accomplish their respective objectives faster with respect to time can reduce the settling time further. Hence, the paper concludes that the supervisor's detection time and the switching controllers' performances are the key parameters for evaluating the complete control strategy's performance.

## 6.2 Optimal control

Paper F examines an optimal linear control strategy implemented as a Proportional–Integral–Derivative controller with low-pass filter (PIDF) controller

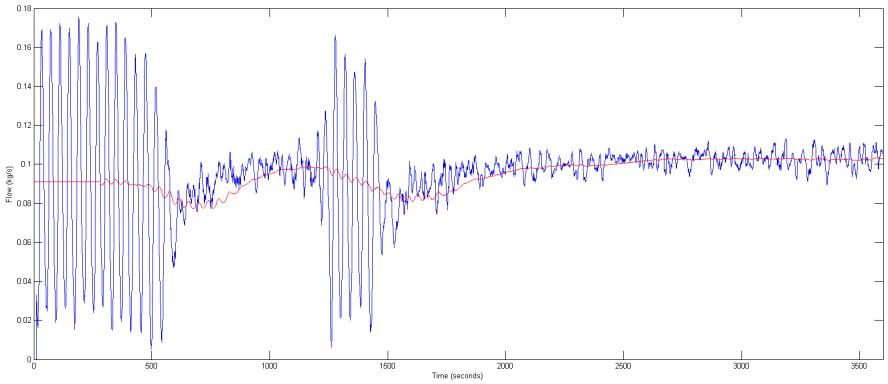


**Fig. 17:** Figure from Paper E showing the mass outflow response for the proposed supervisory $P_b$ controller. The controller is activated at 200 seconds. The blue line is the measured mass flow rate, and the red line is the average mass flow rate over 200 seconds.

with the following structure:

$$K_{PIDF}(s) = K_p(1 + \frac{1}{sT_i} + \frac{T_d s}{T_f s + 1}) \tag{74}$$

where $K_p$ is the proportional gain, $T_i$ is the integral time, $T_d$ is the derivative time and $T_f$ is the time constant of the derivative filter. The filter is essential for reducing the noise effect to the derivative part.

The controller has been automatically tuned by using an optimization algorithm on the linearized model to minimize the weighted sum of a designed cost function ($J(t)$) for the closed-loop input and output performance, such that the optimization problem finds the minimum $J(t)$ by manipulating $K_{PIDF}$ using the Integrated Square Error (ISE). The cost function is shown in equation (76) and is obtained by applying the cost from the ISE function in equation (75) and adding an extra cost parameter $|\dot{u}(t)|$:

$$ISE = \int_0^\infty (r(t) - y(t))^2 dt \tag{75}$$

$$\min_{K_{PIDF}} J(t) = \min_{K_{PIDF}} \int_0^\infty \left( w_y (r(t) - y(t))^2 + w_{u,dif} \left| \dot{u}(t) \right|^2 \right) dt \tag{76}$$

where r is the output reference, and $w_y$ and $w_{u,dif}$ are weighting values. $w_y$ has the highest weighting prioritization over $w_{u,dif}$ which is adjusted to take care of the physical rate limiter for the choke valves opening speed.

A convex optimization solver (IPOPT) is used for finding the cost function's optimum, where the Jahanshahi-Skogestad model is linearized by Jaco-

bian linearization to obtain a linear model. In this way, the solver's estimated optimum will in fact be the global optimum for the simplified model.

| Open-loop $Z_{bif} = 23\%$* | Non-linear MATLAB model | | | OLGA model | | | |
|---|---|---|---|---|---|---|---|
| Measurement | Optimal PIDF | IMC -PIDF | $H_\infty$ Loop-shaping | Optimal $PIDF_{MATLAB}$ | Tuned $PIDF_{OLGA}$ | IMC -PIDF | $H_\infty$ Loop-shaping |
| $P_b$ [bar] | 62 % | 70 % | 98 % | 46 % | 59 % ** | 47 % | 74 % |
| $P_t$ [bar] | - | - | 35 % | - | 29 % ** | - | 41 % |

**Table 6:** Table from Paper F showing the controller comparison between $P_b$ and $P_t$ with optimal PIDF, IMC-PIDF and $H_\infty$ loop-shaping control schemes. The table's result entries show the absolute maximum stable choke opening indicating the closed-loop bifurcation point for each controller respectively.

* The open-loop $Z_{bif}$ is 23.3 % in OLGA and 23.6 % in MATLAB

** The controller has been retuned in OLGA to obtain better results.

In Paper F the results show that the linear optimal PIDF control strategy performed relatively badly compared with other examined control strategies. This can be seen in table 6 from paper F, where both MATLAB and OLGA simulations show the respective closed-loop bifurcation points for each of the examined controllers. It is clear that the optimal PIDF controller performs badly both in the MATLAB and OLGA, and that the strategy could not eliminate the slug outside the open-loop bifurcation point for $P_t$. It is suspected that this is caused by the model linearization stage, where the model might lose some accuracy and that the linearized model's optimum deviates significantly from the actual non-linear model's optimum.

## 6.3 Internal Model Control (IMC)

Another controller examined in Paper F is a Internal Model Control (IMC) PIDF controller, where the traditional IMC structure is rewritten into a linear PIDF structure. The methods for rewriting the IMC into a IMC-PIDF control scheme are examined in [144]. In Paper F the model is linearized which results in a second order transfer function with time delay, see equation (77).

$$G(s) = \frac{ke^{-\theta s}}{(\tau_1 s + 1)(\tau_2 s + 1)} \tag{77}$$

This model is used for estimating the respective P, I and D control parameters as shown in equation (78), (79) and (80). The filter is manually added to the derivative part after the P, I and D values are obtained.

$$K_p = \frac{1}{k}\frac{\tau_1}{\tau_c + \theta} \tag{78}$$

$$T_i = min(\tau_1, 4(\tau_c + \theta)) \tag{79}$$

$$T_D = \tau_2 \tag{80}$$

$\tau_c$ is the only tuning parameter and $\tau_c \approx \theta$. Table 6 shows that the IMC-PIDF controller performs better than the optimal PIDF controller. However, for $P_t$ the IMC-PIDF controller can not eliminate the slug above the open-loop bifurcation point. Like for the optimal PIDF controller, the bad controller performance is suspected to be caused by the linearization where the model might lose too much information for effective anti-slug control. Furthermore, model reduction is used, where the *half rule* from [144] is applied, such that the two zeros from the original linearized model is reduced to a time delay ($\theta$). This model simplification can also have been a reason for the relatively bad controller performance with the non-linear models.

## 6.4 Robust control

Robust control is a branch of control theory which handles design of controllers by explicitly dealing with uncertainties [147]. The robust control methods are designed to achieve an acceptable robust performance and stability, provided that the uncertain parameters and/or disturbances are found within some bounded set [148]. Robust controllers are static and thus does not adapt to variations (unlike adaptive controllers), which can be useful if the given model uncertainties are unknown but bounded.

Robustness to parametric and input disturbances is a desired feature for anti-slug controllers, as the slug's chaotic behavior often challenges the accuracy of the controller, due to the model uncertainties, which can change the closed-loop performance significantly [64,65]. For this reason robust controllers have proven effective for eliminating the slugs in uncertain conditions [63, 104, 149]. The cost for robustifying the system is the performance for the closed-loop performance for the nominal plant. Thus a trade-off between nominal performance and robustness have to be made for any robust control scheme.

### 6.4.1 H-infinity Loop-shaping

There are many different robust controllers, and in [63] a comparison between different anti-slug controllers was carried out, and it was concluded that the $H_\infty$ Loop-shaping controller performed well for slug tasks. For this reason the controller comparison in Paper F also includes the $H_\infty$ Loop-shaping control strategy.

$H_\infty$ loop-shaping is based on the perturbed plant model $G_p$ to maximize the stability margin for model uncertanties. The normalized left coprime factorization of $G$ is

$$G = M^{-1}N. \tag{81}$$

For simplification, the subscript of $M$ and $N$ is not included. Hence, the perturbed plant model is

$$G_P = (M + \Delta M)^{-1}(N + \Delta N). \tag{82}$$

Here $\Delta M$ and $\Delta N$ are stable transfer functions which represent the uncertainty in the nominal plant model. The controller's objective is to stabilize a list of perturbed plants, defined by

$$G_P = \left\{ (M + \Delta M)^{-1}(N + \Delta N) \ : \ \|[\Delta N \ \Delta M]\|_\infty < \epsilon \right\} \tag{83}$$

Hence, the closed-loop feedback system is stable if and only if the nominal feedback system is stable and

$$\gamma_K \stackrel{\Delta}{=} \left\| \begin{bmatrix} K \\ I \end{bmatrix} (I - GK)^{-1} M^{-1} \right\|_\infty \leq \frac{1}{\epsilon} \tag{84}$$

where $\epsilon > 0$ is the stability margin and $\gamma_K$ is the $H_\infty$ norm. When $\gamma_K$ is small the stability margin, $\epsilon$, is equivalently large. Now $K$ can be obtained by solving two algebraic Riccati equations [63].

In table 6 it is clearly observed that the $H_\infty$ loop-shaping controller gives the largest closed-loop bifurcation points for both $P_b$ and $P_t$ in both MATLAB and OLGA simulations. An interesting observation, which is not included in Paper F, is that the classical loop-shaping (before the robustification) performs worse than the $H_\infty$ loop-shaping controller in most of the considered simulation results, although the classical loop-shaping obviously performs best for the linearized nominal plant. This indicates that the bounded model uncertainties included in the $H_\infty$ control design are an improved description of the model when the linearized model is used for the control design.

## 6.5 Discussion

The considered controllers show that a self-learning supervisory controller can operate close to the closed-loop system's stable boundaries and that the supervisor is not restricted to a specific controller. The limitation is the supervisor's detection time, which can be improved by reducing the slug supervisor's detection threshold value. Essentially, the determination of the threshold is a trade-off between detection time and sensitivity to false detections.

The supervisory control scheme can operate in combination with all the controllers examined in chapter 6.2, 6.3, and 6.4.1. From the considered control simulations, the $H_\infty$ Loop-shaping controller performs well in an uncertain environment while the nominal performance also is acceptable. However, the stability margin has to be robustified significantly when large model uncertainties are present.

# 7 Electrical Resistance Tomography (ERT)

Paper D examines an alternative measurement principle for slug detection based on experiments with a new transmitter. The proposed transmitter is based on a tomography principle which measures the electrical resistance over a pipeline's cross area section; Electrical Resistance Tomography (ERT). Furthermore, the paper also investigates how the ERT can operate as the measurement in a feedback control strategy. A fast slug detection method is motivated by the supervisory control strategy examined in Paper E, where it is concluded that a fast slug detection is critical for a reduced settling time.

The ERT principle over a pipeline can be observed in figure 18 from paper D. During the first sample the first probe is actively sending out a current signal over the pipeline cross area section. This is illustrated by the red line. During the second sample the second active probe is providing the current signal and the blue line indicates the signal running through the pipeline during that sample. It is clear that when the probes are active in turns, and the rest of the probes are passive, receiving the signal from the active probe. Thus, after all probes have been active once, a grid over the pipeline cross area section can be visualized. The grid resolution is depending on the total number of probes.

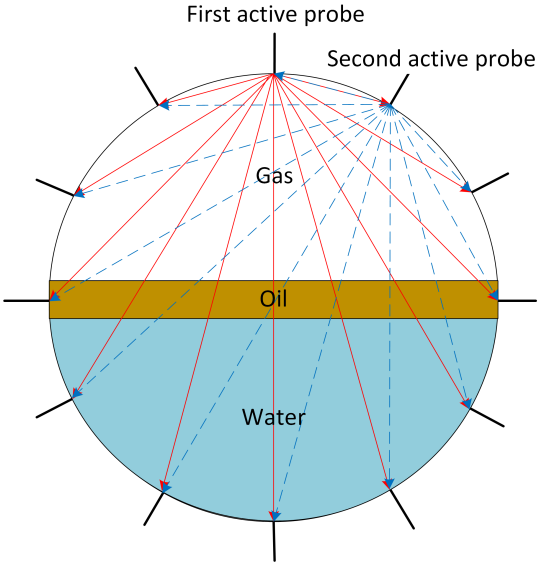


**Fig. 18:** Figure from Paper D. The cross area section of a 3-phase pipeline with the 12 probes, where it is shown how the probes in turn switches between being active, while the rest are passive.

The experimental stand-alone testing facility is a closed flow loop and is shown in figure 19 from Paper D and the ERT transmitter can be observed in figure 20b. The stand-alone testing facility has inflow pumps, valves and multi-phase meters for the water and gas installed, respectively. Furthermore, pressure measurements are installed up- and downstream the ERT transmitter and a coriolis flow meter is installed downstream the ERT transmitter for measureing the multi-phase flow. The ERT transmitter itself consists of 12 probes installed on a transparent PVC pipeline, and hence 12 samples are required for one cross area section map. The map consists of 132 measurements and the sampling frequency is 1000 Hz. Thus a cross area section map can be obtained with a frequency of 83 Hz, which is sufficient for monitoring the multi-phase flow dynamics. The data acquisition (DAQ) is achieved through Simulink Real-Time similarly as in chapter 3.4.

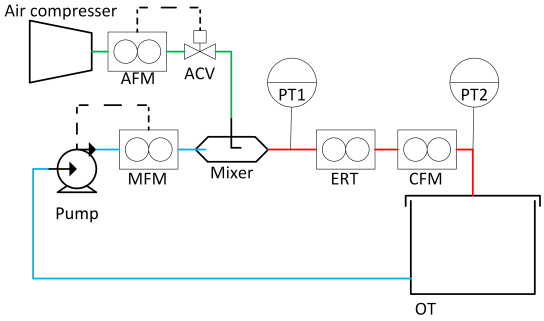


**Fig. 19:** Figure from Paper D. A P&ID diagram of the stand-alone multi-phase testing facility for examining new equipment.

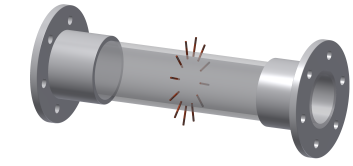

**(a)** A 3D drawing of the pipeline with the 12 ERT probes.

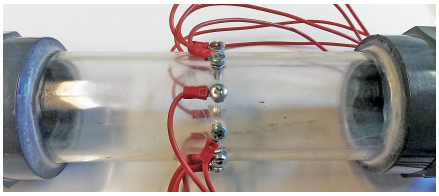

**(b)** A photo of the transparent PVC pipeline where the ERT transmitter is installed. Red wires are connected to each of the 12 probes.

**Fig. 20:** The experimental ERT transmitter on a horizontal pipeline.

The results are obtained based on water and air 2-phase experiments,

and thus the oil phase is not included. It has to be presumed that the liquid phases are well-mixed (the oil and water is one homogenious media) and the oil-to-water ratio is low. The experiments in Paper D show that the the average resistance over the pipeline cross area section measured by the ERT transmitter can identify different slug cycles. The ERT measurements can detect the slug independently of the slug frequencies and faster than the topside pressure transmitter. However, the ERT is more sensitive to the gas penetration, especially during the gas blow-out. The ERT transmitter's ability to detect slug is observed to be equivalent to the flow meter. Paper D concludes that the results indicate that the ERT principle can be an effective method to detect the slug, but not necessarily better than a topside pressure transmitter.

# 8 Impact on separation performance

Paper G investigates how the severe riser-induced slugs influence the traditional downstream separation process. Figure 4 shows the traditional de-oiling configuration on offshore platforms, consisting of a 3-phase gravity separator and a de-oiling hydrocyclone physically linked to the gravity separator's water outlet. The 3-phase gravity separator separates the gas from liquid, and most of the oil from water. In this way the gravity separator has one multi-phase inlet and three single-phase outlets. However, the produced water at the water outlet cannot be discharged directly into the ocean when the produced water includes more than the legal hydrocarbon discharge restrictions [105,109,110]. For this reason a downstream de-oiling hydrocyclone is installed to separate the oil from the water down to below the legal threshold value. This configuration is emulated in the 3rd generation test facility (see section 3.3). Thus, different pipeline-riser flow regimes are tested in Paper G, to observe the relationship between the riser-induced slugs and the separation performance.

A water level controller is implemented on the gravity separation. Here, the inflow's relationship to the water outlet is critical to the downstream hydrocyclone, as the inflow can be manipulated by a topside choke valve and the outflow feeds the hydrocyclone. Assuming all other running conditions are constant and the initial water level is equal to the controller reference ($level_{w,init} = ref_{w,level}$), if a perfect (infinity fast) water level controller is installed in a gravity separator, the separator's water mass inflow ($\omega_{sep,l,in}$) will at any point in time be equal to the separator's water mass outflow ($\omega_{sep,w,out}$). In reality there will be a time delay between the in- and outflow fluctuations.

Paper G considers several scenarios with no, open-loop, and closed-loop anti-slug control strategies, using the choke valve at the topside riser. The

overall conclusion is that the severe riser-induced slugs play a significant role in the performance of both the gravity separator's water level and the hydrocyclone's pressure drop ratio (PDR) controllers' tracking abilities. Hence, the paper confirms that a stable separator inflow is crucial for acceptable PDR setpoint tracking. When slugs enter the gravity separator, the level controller tries to maintain the water level's reference point, and thus the water outlet flow varies equivalently to the inlet flow with subject to amplitude and frequency. Hence, the hydrocyclone's inlet flow will also vary proportionally to the gravity separator's inlet flow. It is experimentally observed that the PDR controller easily saturates the hydrocyclone's overflow valve, and correspondingly cannot track the PDR reference point.

Figure 21 from Paper G shows a comparison between the PDR's steady-state distribution of no, open-loop and closed-loop anti-slug control solutions for scenario 2 in paper G. It is clear that the open- and closed-loop control strategies both result in narrower PDR values than for the fully open case. It indicates that the non-slugging flow regime will cause smaller fluctuations in the PDR value. It can also be noted that there is an offset in PDF peaks from the PDR setpoint which is caused by the saturation of the overflow valve.

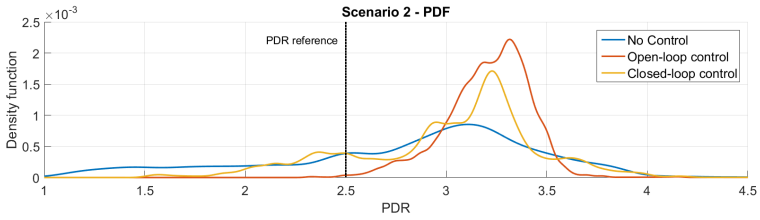


**Fig. 21:** Figure from paper G. The pressure drop ratio's (PDR) steady-state distribution comparison between no, open-loop and closed-loop anti-slug control solutions for scenario 2 in paper G.

The overall conclusion in Paper G is that the elimination of severe riser-induced slugs is important for acceptable PDR tracking, due to the gravity separator's and the de-oiling hydrocyclone's sensitivity to the gravity separator's inflow. The separation efficiency is not measured and thus it is hard to determine the riser-induced slugs' exact effect to the de-oiling efficiency. However, it is observed that the hydrocyclone overflow valve saturated when the PDR fluctuated too much, which is undesired for the separation performance.

# 9 Conclusion

This thesis considers the severe slugs in offshore multi-phase well-pipeline-riser processes in oil & gas installations; the physical phenomenon, the challenges that arises with the severe slugs, a theoretical and experimental open- and closed-loop process investigation, slug elimination and anti-slug control strategies, as well as instrumentation and equipment analysis.

The main contributions in this thesis lies within the state-of-the-art and future challenges in Paper A and B, the open-loop system analysis in Paper C, the transmitter investigation in Paper D, the new-proposed supervisory control strategy in Paper E, the IO controllability and control comparison in Paper F, and the examination of severe slugs effect to the downstream separation processes in Paper G.

In Paper A and B the severe slugs in well-pipeline-riser processes is examined. Based on a detailed literature review it is concluded that the main problem with existing anti-slug control strategies is the lack of robustness to the changing and uncertain process running conditions. Furthermore, it is concluded that the worldwide severity rate of the slugs will increase in the future due to the deeper production wells and risers, as well as the decrease in reservoir pressure at mature wells. Thus, the industry will in the future demand effective and inexpensive ways to eliminate the severe slugs.

Paper C shows that the bifurcation maps and flow maps are dependent on information from each other. Hence, a new 3D map is proposed and experimentally investigated. It combines the information of the traditional flow and bifurcation maps, such that the new-proposed map contains more information than the existing respective methods. The map can be applied by operators for a full process understanding, both considering the flow rates and the manipulation variables. Furthermore, the 3D map can be used for closed-loop cases as well, which significantly improves the applicability for control engineers.

In Paper D an ERT transmitter is implemented on a closed flow loop test facility emulating a topside horizontal platform. The ERT is considered a cost-effective slug detection alternative to the existing measurements on offshore oil & gas installations. The paper's results show that the ERT method, using the average electrical resistance over the cross area section, can detect severe slugs better than a topside pressure transmitter, when the multi-phase flow is well-mixed and the oil-to-water ratio is low. However, it is also concluded that the gas surge stage causes fluctuation in the ERT measurements, which is hard to distinguish from no production rate (where the is little liquid in the topside section). For this reason it is concluded that the average resistance over the pipeline cross area section is not necessarily a better slug detection option than the existing transmitters, such as topside flow meter

or pressure transmitter. However, other image processing methods might improve the detection reliability of the ERT technique.

In Paper E a supervisory control strategy is proposed, with a self-learning reference procedure and a switching control structure. The supervisor's objective is to detect the slug in a fast and reliable manner, the self-learning reference procedure aims at finding the optimal operation point based on the supervisor's decision, and the switching between two controllers are implemented for (i) eliminating the slug, and (ii) optimizing the production. It is concluded that the entire control strategy improves the production rate significantly and that the self-learning reference does not demand the offshore operator to pick a reference point. However, the strategy is limited by the detection time of the supervisor as well as the performance of each of the switching controllers, respectively.

In Paper F a IO controllability analysis is carried out to examine several system outputs, respectively. $P_t$ can eliminate severe slugs, but not at large valve openings. Instead $P_{in}$, $P_b$, and $\omega_{out}$ all seem to be better for anti-slug control outputs. That is also observed in simulations in the non-linear MATLAB and OLGA simulations where all examined control strategies with $P_b$ perform better than with $P_t$. Furthermore, $H_\infty$ loop-shaping performs better than the examined optimal PIDF and IMC-PIDF, both with and without included input and parametric disturbances.

Paper G investigates the slugs' effect on the downstream separation efficiency. The traditional PWT separation facilty, consisting of a gravity separator and a de-oiling hydrocyclone, is influenced by especially the varying mass inflow to the separator. The fluctuating flow is sent directly through the separator to the downstream hydrocyclone at the water outlet due to the implemented water level controller. The hydrocyclone's PDR controller is easily saturated when the inflow is varying. All in all the occurrence of severe slugs heavily reduces the PWT separation process' efficiency.

The overall conclusion is that designing an effective anti-slug control strategy is a complicated task, but essential for consistent production operation, as the severe slug both significantly reduces the production rate and complicates the downstream separation process. Supervisory control can be an effective anti-slug stategy if a fast and reliable detection algorithm is implemented. $P_t$ can be used as measurement in riser-induced anti-slug control schemes, however $P_{in}$, $P_b$, and $\omega_{out}$ are all better alternatives. Furthermore, a robust controller strategy, such as $H_\infty$ loop-shaping, seems to be an effective approach for handling the uncertain operating process conditions as the low-dimensional models often lack some accuracy due to the chaotic behavior of the severe slugs. It can also be concluded that a sub-optimal controller can be preferable, as operation with large valve openings reduces the closed-loop systems' robustness while not improving the production rate significantly.

# References


[1] Zhenyu Yang, Simon Pedersen, and Petar Durdevic. Cleaning the Produced Water in Offshore Oil Production by Using Plant-wide Optimal Control Strategy. *Proceedings of the OCEANS'14 MTS/IEEE Conference*, 2014.

[2] Petar Durdevic, Leif Hansen, Christian Mai, Simon Pedersen, and Zhenyu Yang. Cost-Effective ERT Technique for Oil-in-Water Measurement for Offshore Hydrocyclone Installations. *Proceedings of the 2nd IFAC Workshop on Automatic Control in Offshore Oil and Gas Production*, 48(6):147–153, 2015.

[3] Petar Durdevic, Simon Pedersen, Mads Valentin Bram, Dennis S. Hansen, Abdiladif Ahmed Hassan, and Zhenyu Yang. Control oriented modeling of a de-oiling hydrocyclone. *Proceedings of the 17th IFAC Symposium on System Identification*, 48(28):291–296, 2015.

[4] Mads V Bram, Abdiladif A Hassan, Dennis S Hansen, Petar Durdevic, Simon Pedersen, and Zhenyu Yang. Experimental modeling of a deoiling hydrocyclone system. In *Proceedings of the 20th International Conference on Methods and Models in Automation and Robotics (MMAR)*, pages 1080–1085. IEEE, 2015.

[5] Petar Durdevic, Simon Pedersen, and Zhenyu Yang. Evaluation of OiW Measurement Technologies for Deoiling Hydrocyclone Efficiency Estimation and Control. *Proceedings of OCEANS'16 MTS/IEEE, Shanghai*, 2016.

[6] Petar Durdevic, Simon Pedersen, and Zhenyu Yang. Efficiency control in offshore de-oiling installations. *Submitted to Computers and Chemical Engineering*, 2016.

[7] Zhenyu Yang, Simon Pedersen, and Petar Durdevic. Control of Variable-Speed Pressurization Fan for an Offshore HVAC System. *Proceedings of the 2014 IEEE International Conference on Mechatronics and Automation (ICMA)*, pages 458–463, 2014.

[8] Petar Durdevic, Simon Pedersen, and Zhenyu Yang. Modeling Separation Dynamics in a Multi-Tray Bio-Ethanol Distillation Column. *Proceedings of the 2015 IEEE International Conference on Mechatronics and Automation (ICMA)*, pages 1349–1354, 2015.

[9] Y. Taitel, D. Barnea, and A. E. Dukler. Modeling flow pattern transitions for steady upward gas–liquid flow in vertical tubes. *AIChE Journal*, 26(3):345–354, 1980.

[10] Eissa M. Al-safran, Yehuda Taitel, and James P. Brill. Prediction of slug length distribution along a hilly terrain pipeline using slug tracking model. *Journal of Energy Resources Technology, Transactions of the ASME*, 126:54–62, 2004.

[11] Heidi Sivertsen, Espen Storkaas, and Sigurd Skogestad. Small-scale experiments on stabilizing riser slug flow. *Chemical Engineering Research and Design*, pages 213–228, 2010.

[12] Z.G. Xu and M. Golan. Criteria for operation stability of gas lift. *SPE 19362*, 1989.

[13] Laure Sinègre, Nicolas Petit, and Philippe Menegatti. Distributed delay model for density wave dynamics in gas lifted wells. *IEEE Conference on Decision and Control, and the European Control Conference*, 44, 2005.

[14] Luo Xiaoming, He Limin, and Ma Huawei. Flow pattern and pressure fluctuation of severe slugging in pipeline-riser system. *Fluid Flow And Transport Phenomena, Chinese Journal of Chemical Engineering*, 19:26—32, 2011.

[15] Ogazi A. Isaac, Yi Cao, Liyun Lao, and Hoi Yeung. Production potential of severe slugging control systems. *18th IFAC World Congress*, pages 10869–10874, 2011.

[16] Bin Hu and Michael Golan. Characterizing gas-lift instabilities by dynamic simulation. *2-Fall Gas-Lift Workshop, Kuala Lumpur, Malaysia*, 2003.

[17] Bin Hu. *Characterizing gas-lift instabilities*. PhD thesis, Norwegian University of Science and Technology (NTNU), Department of Petroleum Engineering and Applied Geophysics, 2004.

[18] Kjetil Havre, Karl Ole Stornes, and Henrik Stray. Taming slug flow in pipelines, 2000.

[19] Ingvald Baardsen. Slug regulering i tofase stroemning - eksperimentell verifikasjon. Master's thesis, Norwegian University of Science and Technology, 2003.

[20] T. J. Hill and D. G. Wood. Slug flow: Occurrence, consequences, and prediction. *University of Tulsa Centennial Petroleum Engineering Symposium*, 1994.

[21] Zhenyu Yang, Jens Peter Stigkær, and Bo Løhndorf. Plant-wide control for better de-oiling of produced water in offshore oil & gas production. *3rd IFAC International Conference on Intelligent Control and Automation Science*, 3:45–50, 2013.

[22] Zhenyu Yang, Michael Juhl, and Bo Løhndorf. On the innovation of level control of an offshore three-phase separator. *2010 IEEE International Conference on Mechatronics and Automation*, pages 1348–1353, 2010.

[23] Mathias Wilhelmsen. Control structure and tuning method design for suppressing disturbances in a multi-phase separator. Master's thesis, Norwegian University of Science and Technology, Department of Engineering Cybernetics, 2013.

[24] Trygve Husveg, Odile Rambeau, Tormod Drengstig, and Torleiv Bilstad. Performance of a deoiling hydrocyclone during variable flow rates. *Minerals Engineering 20*, pages 368–379, 2007.

[25] J-Y. Sun and W. P. Jepson. Slug flow characteristics and their effect on corrosion rates in horizontal oil and gas pipelines. *SPE 24787*, pages 215–228, 1992.

[26] X. Zhou and W. P. Jepson. Corrosion in three-phase oil/water/gas slug flow in horizontal pipes. *NACE International*, page Paper no. 26, 1994.

[27] C. Kang, R. Wilkens, and W. P. Jepson. The effect of slug frequency on corrosion in high pressure, inclined pipelines. *NACE International*, page Paper no. 20, 1996.

[28] Lanchang Xing, Hoi Yeung, Joseph Shen, and Yi Cao. A new flow conditioner for mitigating severe slugging in pipeline/riser system. *International Journal of Multiphase Flow*, 51:65–72, 2013.

[29] B.T. Yocum. Offshore riser slug flow avoidance: Mathematical model for design and optimization. *SPE 4312, London, UK*, 1973.

[30] A. G. Adedigba. *Two-phase flow of gas–liquid mixtures in horizontal helical pipes*. PhD thesis, Cranfield University, 2007.

[31] Lanchang Xing, Hoi Yeung, Joseph Shen, and Yi Cao. Numerical study on mitigating severe slugging in pipeline/riser system with wavy pipe. *International Journal of Multiphase Flow*, 53:1–10, 2013.

[32] Lanchang Xing, Hoi Yeung, Joseph Shen, and Yi Cao. Experimental study on severe slugging mitigation by applying wavy pipes. *Chemical Engineering Research and Design*, 91:18–28, 2013.

[33] Brook Makogan. Patent on device for controlling slugging. http://patentscope.wipo.int/search/en/WO2007034142, 2007.

[34] C. Sarica and J. Ø. Tengesdal. A new technique to eliminate severe slugging in pipeline/riser systems. *SPE Annual Technical Conference & Exhibition, SPE 63185*, pages 633–641, 2000.

[35] J. O. Tengesdal, C. Sarica, and L. Thompson. Severe slugging attenuation for deepwater multiphase pipeline and riser systems. *PE Annual Technical Conference and Exhibition, Paper SPE 87089*, 2002.

[36] A.R. Almeida and M.A.L. Gonçalves. Device and method for eliminating severe slugging in multiphase-stream flow lines. Patent: US6041803A, 1999.

[37] A.R. Almeida and M.A.L. Gonçalves. Venturi for severe slugging elimination. *The 9th International Conference on Multiphase Production*, pages 149–158, 1999.

[38] F. E. Jansen, O. Shoham, and Y. Taitel. The elimination of severe slugging - experiments and modeling. *Int. J. Multiphase Flow*, 22:1055–1072, 1996.

[39] T. Hassanein and P. Fairhurst. Challenges in the mechanical and hydraulic aspects of riser design for deep water developments. *IBC UK Conf. Ltd. Offshore Pipeline Technology Conference*, 1998.

[40] M. McGuiness and D. Cooke. Partial stabilization at st. joseph. *Proceeding of the 3rd International Offshore and Polar Engineering Conference*, pages 235–241, 1993.

[41] Kjetil Havre and Morten Dalsmo. Active feedback control as the solution to severe slugging. *SPE Annual Technical Conference & Exhibition, New Orleans, Louisiana*, 2001.

[42] A.I. Ogazi, Y. Cao, H. Yeung, and L. Lao. Slug control with large valve openings to maximize oil production. *Society of Petroleum Engineers (SPE), Offshore Europe Oil & Gas Conference & Exhibition held in Aberdeen, UK*, Volume 15, Number 3, 2010.

[43] Anayo Isaac Ogazi. *Multiphase Severe Slug Flow Control*. PhD thesis, Cranfield University, School of Engineering, Department of Offshore, Process and Energy Engineering, 2011.

[44] Esmaeil Jahanshahi. *Control Solutions for Multiphase Flow : Linear and nonlinear approaches to anti-slug control*. PhD thesis, Norwegian University of Science and Technology, Department of Chemical Engineering, 2013.

[45] G.O. Eikrem, O.M. Aamo, H.B. Siahaan, and B.A. Foss. Anti-slug control of gas-lift wells - experimental results. *6th IFAC Symposium on Nonlinear Control Systems, Stuttgart, Germany*, 2004.

[46] G. O. Eikrem. *Stabilization of gas-lift wells by feedback control*. PhD thesis, Department of Engineering Cybernetics, Norwegian University of Science and Technology, 2006.

[47] Kasper Jepsen, Leif Hansen, Christian Mai, and Zhenyu Yang. Emulation and control of slugging flows in a gas-lifted offshore oil production well through a lab-sized facility. *IEEE International Conference on Control Applications (CCA)*, pages 906–911, 2013.

[48] M.R. Mahdiani and E. Khamehchi. Preventing instability phenomenon in gas-lift optimization. *Iranian Journal of Oil & Gas Science and Technology*, 4:49–65, 2015.

[49] V. de Oliveira, J. Jäschka, and S. Skogestad. An autonomous approach for driving systems towards their limit: An intelligent adaptive anti-slug control system for production maximization. *2nd IFAC Workshop on Automatic Control in Offshore Oil and Gas Production, Florianopolis, Brazil*, pages 104–111, 2015.

[50] Esmaeil Jahanshahi, Sigurd Skogestad, and Anette H. Helgesen. Controllability analysis of severe slugging in well-pipeline-riser systems. *IFAC Workshop on Automatic Control in Offshore Oil and Gas Production, NTNU, Trondheim, Norway*, pages 101–108, 2012.

[51] B. Foss. Process control in conventional oil and gas field - challenges and opportunities. *Control Engineering Practice 20, 4th Symposium on Advanced Control of Industrial Processes (ADCONIP)*, pages 1058 – 1064, 2012.

[52] S. Mokhatab and B. F. Towler. Severe slugging in flexible risers: Review of experimental investigations and olga predictions. *Petroleum Science and Technology*, 25:867–880, 2007.

[53] Saeid Mokhatab. *Severe slugging in offshore production systems*. Nova Science Publishers, Inc., 2010.

[54] Saeid Mokhatab and William A. Poe. *Handbook of Natural Gas Transmission and processing*. Gulf professional Publishing, 2012.

[55] Florent Di Meglio, Glenn-Ole Kaasa, Nicolas Petit, and Vidar Alstad. Model-based control of slugging: Advances and challenges. *2012 IFAC Workshop on Automatic Control in Offshore Oil and Gas Production*, pages 109–115, 2012.

[56] Simon Pedersen, Petar Durdevic, and Zhenyu Yang. Review of slug detection, modeling and control techniques for offshore oil & gas production processes. *2nd IFAC Workshop on Automatic Control in Offshore Oil and Gas Production*, 48:89–96, 2015.

[57] Simon Pedersen, Kasper Stampe, Sandra Lindberg Pedersen, Petar Durdevic, and Zhenyu Yang. Experimental Study of Stable Surfaces for Anti-Slug Control in Multi-phase Flow. *International Conference on Automation & Computing, Cranfield University*, 20:43–48, 2014.

[58] Jakob Biltoft, Lasse Hansen, Simon Pedersen, and Zhenyu Yang. Recreating riser slugging flow based on an economic lab-sized setup. *IFAC International Workshop on Periodic Control*, 5th:47–52, 2013.

[59] Anette Hoel Helgesen. Anti-slug control of two-phase flow in risers with: Controllability analysis using alternative measurements. Master's thesis, NTNU, Norway, 2010.

[60] R. A. Williams, X. Jia, R. M. West, M. Wang, J. C. Cullivan, J.Bond, I. Faulks, T. Dyakowski, S. J. Wang, N. Climpson, J. A. Kostuci, and D. Payton. Industrial monitoring of hydrocyclone operation using electrical resistance tomography. *Minerals Engineering*, 12(10), 1999.

[61] M. A. Bennett, R. M. West, S. P. Luke, and R. A. Williams. The investigation of bubble column and foam processes using electrical capacitance tomography. *Minerals Engineering*, page 225–234, 2002.

[62] M. A. Bennett and R. A. Williams. Monitoring the operation of an oil/water separator using impedance tomography. *Minerals Engineering*, 17, 2004.

[63] E. Jahanshahi, V. De Oliveira, C. Grimholt, and S. Skogestad. A comparison between internal model control, optimal pidf and robust controllers for unstable flow in risers. *19th World Congress, The International Federation of Automatic Control (IFAC'14)*, pages 5752–5759, 2014.

[64] Jayaprakash Sivasamy, Zhizhao Che, Teck Neng Wong, Nam-Trung Nguyen, and Levent Yobas. A simple method for evaluating and predicting chaotic advection in microfluidic slugs. *Chemical engineering science*, 65(19), 2010.

[65] Zhong-Ke Gao and Ning-De Jin. Characterization of chaotic dynamic behavior in the gas–liquid slug flow using directed weighted complex network analysis. *Physica A: Statistical Mechanics and its Applications*, 391(10):3005 – 3016, 2012.

[66] K.H Bendiksen, D. Malnes, R. Moe, and S. Nuland. *Information for beginning with OLGA - "The dynamic Two-Fluid Model OLGA: Theory and application"*. SPE Production Engineering, 2013.

[67] Kongsberg. *LedaFlow® - The new multiphase simulator. User guide (2014)*, 2014.

[68] Thomas J. Danielson, Kris M. Bansal, Biljana Djoric, Emmanuel Duret, and Stein Tore Johansen. Testing and qualification of a new multiphase flow simulator. *Offshore Technology Conference, Houston, Texas.*, 2011.

[69] R. Belt, B. Djoric, S. Kalali, E. Duret, and D. Larrey. Comparison of commercial multiphase flow simulators with experimental and field databases. *BHR Group's Multiphase Production Technology Conference in Cannes*, 15, 2011.

[70] Espen Storkaas, Sigurd Skogestad, and John-Morten Godhavn. A low-dimensional dynamic model of severe slugging for control design and analysis. *11th International Conference on Multiphase flow (Multiphase '03)*, pages 117–133, 2003.

[71] Esmaeil Jahanshahi and Sigurd Skogestad. Simplified dynamical models for control of severe slugging in multiphase risers. *18th IFAC World Congress*, pages 1634–1639, 2011.

[72] G. O. Eikrem. Eikrem riser model. http://www.nt.ntnu.no/users/skoge/diplom /prosjekt08/tuvnes/Eikrem_ risermodel_ matlab/, 2008.

[73] G.-O. Kaasa and et. al. V. Alstad. Attenuation of slugging in unstable oil wells. *Nonlinear Control. 17th IFAC World Congress, Seoul, Korea*, 2008.

[74] C. M. Da Silva and O.J. Nydal. Dynamic multiphase flow models for control. *BHRG North American Conference on Multiphase Technology. Banff, Canada*, 7th, 2010.

[75] Florent Di Meglio, Glenn-Ole Kaasa, and Nicolas Petit. A first principle model for multiphase slugging flow in vertical risers. *Joint 48th IEEE Conference on Decision and Control and 28th Chinese Control Conference*, pages 8244–8251, 2009.

[76] Florent Di Meglio, Nicolas Petit, Vidar Alstadb, and Glenn-Ole Kaasab. Stabilization of slugging in oil production facilities with or without upstream pressure sensors. *Journal of Process Control*, 22:809–822, 2012.

[77] Esmaeil Jahanshahi and Sigurd Skogestad. Simplified dynamic models for control of riser slugging in offshore oil production. *Society of Petroleum Engineers (SPE 172998)*, pages 40–55, 2014.

[78] E. Storkaas and S. Skogestad. Controllability analysis of two-phase pipeline-riser systems at riser slugging conditions. *Control Engineering Practice*, 15:567–581, 2008.

[79] E. Storkaas. *Anti-slug control in pipeline-riser systems*. PhD thesis, Norwegian University of Science and Technology, 2005.

[80] P. Hedne and H. Linga. Suppression of terrain slugging with automatic and manual riser choking. *Advances in Gas-Liquid Flows*, pages 453–469, 1990.

[81] Heidi Sivertsen and Sigurd Skogestad. Cascade control experiments of riser slug flow using topside measurements. *Triennial World Congress, Prague, Czech Republic*, 16th:6, 2005.

[82] Z. Schmidt, J. P. Brill, and H. D. Beggs. Choking can eliminate severe pipeline slugging. *Oil and Gas Journal 12*, pages 230–238, 1979.

[83] F. E. Jansen. Elimination of severe slugging in a pipeline-riser system. *M.S. Thesis, University of Tulsa*, 1990.

[84] P. D. Molyneux and J. P. Kinvig. Method and apparatus for eliminating severe slugging in a riser of a pipeline includes measuring pipeline pressure and operating a valve. Patent: GB2358205, App. no. GB20000013331 20000602, 2000.

[85] M. A. Fargharly. Study of severe slugging in real offshore pipeline riser-pipe system. *PE Middle East Oil Show, Paper SPE 15726*, 1997.

[86] E. Jahanshahi, S. Skogestad, and E. I. Grøtli. Anti-slug control experiments using nonlinear observers. *American Control Conference (ACC), Washington DC, USA*, pages 1058–1064, 2013.

[87] Bjarne Grimstad and Bjarne Foss. A nonlinear, adaptive observer for gas-lift wells operating under slowly varying reservoir pressure. *19th World Congress, The International Federation of Automatic Control (IFAC'14), Cape Town, South Africa*, pages 2824–2829, 2014.

[88] O.M. Aamo, G.O. Eikrem, H.B. Siahaan, and B.A. Foss. Observer design for gas lifted oil wells. *The 2004 American Control Conference, Boston, USA*, 2004.

[89] O. Aamo, G. Eikrem, H. Siahaan, and B. Foss. Observer design for multiphase flow in vertical pipes with gas-lift - theory and experiments. *Journal of Process Control*, 2004.

[90] Gisle Otto Eikrem, Lars Imsland, and Bjarne Foss. Stabilization of gas lifted wells based on state estimation. *IFAC*, 2004.

[91] Francesco Scibilia, Morten Hovd, and Robert Bitmead. Stabilization of gas-lift oil wells using topside measurements. *IFAC World Congress*, 17:13907–13912, 2008.

[92] Esmaeil Jahanshahi, Sigurd Skogestad, and Esten I. Grøtli. Nonlinear model-based control of two-phase flow in risers by feedback linearization. *IFAC Symposium on Nonlinear Control Systems*, 9th:301–306, 2013.

[93] A. Ogazi, S. Ogunkolade, Y. Cao, L. Lao, and H. Yeung. Severe slugging control through open loop unstable pid tuning to increase oil production. *BHR Group*, pages 17–32, 2009.

[94] Marina Enricone Stasiak, Daniel Juan Pagano, and Agustinho Plucenio. A new discrete slug-flow controller for production pipeline risers. *IFAC Workshop on Automatic Control in Offshore Oil and Gas Production*, pages 122–127, 2012.

[95] Kasper Jepsen, Leif Hansen, and Christian Mai. Modeling and control of an unstable gas-lifted oil-producing well. Technical report, Aalborg University Esbjerg, Department of Energy Technology, 2012.

[96] K.S. Johal, C.E. Teh, and A.R. Cousins. An alternative economic method to riserbase gas lift for deep water subsea oil/gas field developments. *Society of Petroleum Engineers (SPE), Offshore Europe, Aberdeen, United Kingdom*, 1997.

[97] A.R. Cousins and K.S. Johal. Multi purpose riser. Pub. No. EP1022429 A1, Mentor subsea technology services Inc., Houston, Texas, 2000. EP Patent App. EP20000300126.

[98] A. Hunt. Where are we now, where are we going? an operator's perspective,. *Presented at the EPSRC London Meeting*, 1998.

[99] T. J. Hill. Gas-liquid challenges in oil and gas production. *Presented at ASME Fluids Engineering Division Summer Meeting*, 1997.

[100] T. Larsson and S. Skogestad. Plantwide control - a review and a new design procedure. *Modeling, Identification and control*, 21(4):209–240, 2000.

[101] K.S. Johal and A.R. Cousins. Intelligent production riser, 2001. US Patent 6253855.

[102] A. Plucenio, C. A. Ganzaroli, and D. J. Pagano. Stabilizing gas-lift well dynamics with free operating point. *Proceedings of the 2012 IFAC Workshop on Automatic Control in Offshore Oil and Gas Production*, pages 95–100, 2012.

[103] M. Campos, T. R. Takahashi, F. Ashikawa, S. Simoes Neto, O. F. V. Meien, and A. Sant Anna Stender. Advanced anti-slug control for offshore production plants. *2nd IFAC Workshop on Automatic Control in Offshore Oil and Gas Production, Florianopolis, Brazil*, pages 83–88, 2015.

[104] Mahnaz Esmaeilpour Abardeh. Robust control solutions for stabilizing flow from the reservoir: S-riser experiments. Master's thesis, Norwegian University of Science and Technology, Department of Chemical Engineering, 2013.

[105] Ahmadun Fakhru'l-Razi, Alireza Pendashteh, Luqman Chuah Abdullah, Dayang Radiah Awang Biak, Sayed Siavash Madaeni, and Zurina Zainal Abidin. Review of technologies for oil and gas produced water treatment. *Journal of Hazardous Materials*, 170(2–3):530 – 551, 2009.

[106] J. P. Ray and F. R. Engelhardt. *Produced Water: Technological/environmental Issues and Solutions*. Springer, 1992.

[107] Howard Duhon. Produced Water Treatment: Yesterday , Today , and Tomorrow. *Oil and Gas Facilities*, pages 29–31, February 2012.

[108] JT Robinson. An overview of produced water treatment technologies. In *14th Annual International Petroleum Environmental Conference, Houston*, 2007.

[109] The Danish Environmental Protection Agency. Status for den danske offshorehandlingsplan til udgangen af 2009. `http://www.mst.dk/`, January 2016.

[110] A. Sinker. Produced water treatment using hydrocyclones - theory and practical application. *4th International Petroleum Environmental Conference*, 2007.

[111] OLF The Norwegian Oil Industry Association. Zero discharges. `https://www.norskoljeoggass.no/PageFiles/8770/Fact%20sheet%20from%20OLF%20-%20Zero%20discharges.pdf`, 2004. [Online; accessed 20-June-2016].

[112] Paul Ekins, Robin Vanner, and James Firebrace. Zero emissions of oil in water from offshore oil and gas installations: economic and environmental implications. *Journal of Cleaner Production*, 15(13-14):1302–1315, September 2007.

[113] DNV GL Oil & Gas. Håndtering av produsert vann - erfaringer fra norsk sokkel. `http://www.norskoljeoggass.no/Global/2016%20dokumenter/DNV%20GL%20rapport%202015-4277.pdf`, 2015. [Online; accessed 20-June-2016].

[114] Bill Bailey, Mike Crabtree, Jeb Tyrie, Jon Elphick, Fikri Kuchuk, Christian Romano, Leo Roodhart, et al. Water control. *Oilfield Review*, 12(1):30–51, 2000.

[115] Nowakowski A.F., J.C. Cullivan, R.a. Williams, and T. Dyakowski. Application of CFD to modelling of the flow in hydrocyclones. Is this a realizable option or still a research challenge? *Minerals Engineering*, 17(5):661–669, May 2004.

[116] T. Husveg. *Operational Control of Deoiling Hydrocyclones and Cyclones for Petroleum Flow Control: Trygve Husveg*. Avhandling / Universitetet i Stavanger. University of Stavanger, 2007.

[117] MT Thew. Cyclones for oil/water separation. *Encyclopaedia of Separation Science*, 2000.

[118] L. Svarovsky and M.T. Thew. *Hydrocyclones: Analysis and Applications*. Fluid Mechanics and Its Applications. Springer Netherlands, 2013.

[119] P. M. Keyser and T. J. Olson. Control method for hydrocarbon hydrocyclones. US Patent: 8475664 B2, 2013.

[120] D. Wolbert, B.-F. Ma, Y. Aurelle, and J. Seureau. Efficiency estimation of liquid-liquid Hydrocyclones using trajectory analysis. *AIChE Journal*, 41(6):1395–1402, June 1995.

[121] S Schuetz, G Mayer, M Bierdel, and M Piesche. Investigations on the flow and separation behaviour of hydrocyclones using computational fluid dynamics. *International Journal of Mineral Processing*, 73(2-4):229–237, February 2004.

[122] J.C. Cullivan, R.a. Williams, T. Dyakowski, and C.R. Cross. New understanding of a hydrocyclone flow field and separation mechanism from computational fluid dynamics. *Minerals Engineering*, 17(5):651–660, May 2004.

[123] Y. Taitel, S. Vierkandt, O. Shoham, and J. P. Brill. Severe slugging in a riser system: experiments and modeling. *Int. J. Multiphase Flow*, 16:57–68, 1990.

[124] Heidi Sivertsen and Sigurd Skogestad. Anti-slug control experiments on a small-scale two-phase loop. *Computer Aided Chemical Engineering*, 20:1021–1026, 2005.

[125] Shazia Farman Ali. *Two phase flow in large diameter vertical riser*. PhD thesis, Cranfield University, 2009.

[126] Eyamba Ita. Small scale experiments on severe slugging in flexible risers. Master's thesis, Norwegian University of Science and Technology, 2011.

[127] R. Malekzadeh, R.A.W.M. Henkes, and R.F. Mudde. Severe slugging in a long pipeline–riser system: Experiments and predictions. *International Journal of Multiphase Flow*, 46:9–21, 2012.

[128] Nailiang Li, Liejin Guo, and Wensheng Li. Gas–liquid two-phase flow patterns in a pipeline–riser system with an s-shaped riser. *International Journal of Multiphase Flow*, 55:10, 2013.

[129] P. D. Hills. Designing piping for gravity flow. *Chemical Engineering*, pages 111–114, 1983.

[130] T.Z. Hamathy. Velocities of large drops and bubbles in media of infinite or restricted extent. *AIChE Journal*, 6:281–288, 1960.

[131] Y Taitel and A. E. Dukler. A model for predicting flow regime transitions in horizontal and near horizontal gas-liquid flow. *AIChE Journal*, 22:47–55, 1976.

[132] Z. Schmidt, J. P. Brill, and H. D. Beggs. Experimental study of severe slugging in a two-phase flow pipeline riser-pipe system. *SPE Journal*, 20:407–414, 1980.

[133] A. Bøe. Severe slugging characteristics; part i: Flow regime for severe slugging; part ii: point model simulation study. *Selected Topics in Two Phase Flow, NTH, Trondheim, Norway*, 1981.

[134] Y.V. Fairuzov, I. Guerrero-Sarabia, C. Calva-Morales, R. Carmona-Diaz, T. Cervantes-Baza, N. Miguel-Hernandez, and A. Rojas-Figueroa. Stability maps for continuous gas-lift wells: A new approach to solving an old problem. *Society of Petroleum Engineers (SPE) Annual Technical Conference and Exhibition, Houston, Texas*, 2004.

[135] Yehuda Taitel. Stability of severe slugging. *International Journal of Multiphase Flow*, 12:203–217, 1986.

[136] P. Fuchs. The pressure limit for terrain slugging. *BHRA International Conference on Multiphase Flow*, 3rd:65–71, 1987.

[137] B.F.M. Pots, I.G. Bromilow, and M.J.W.F. Konijn. Severe slug flow in offshore flowline/riser systems. *SPE (Society of Petroleum Engineers)*, 2:4:347–356, 1987.

[138] H. Asheim. Criteria for gas-lift stability. *Journal of Petroleum Technology*, 40:1452–1456, 1988.

[139] M. Viggiani, O. Mariani, V. Battarra, A. Annunziato, and U. Bollettini. Pipeline simulation interest group (psig) - a model to verify the onset of severe slugging. *PSIG Annual Meeting*, 1988.

[140] S. Vierkandt. Severe slugging in a pipeline-riser system, experiments and modelling. Master's thesis, The University of Tulsa, 1988.

[141] C. Sarica and O. Shoham. A simplified transient model for pipeline-riser systems. *Chemical Engineering Science*, 46:2167–2179, 1991.

[142] J.A. Montgomery. *Severe Slugging and unstable flows in an S-shaped riser*. PhD thesis, Cranfield University, England, 2002.

[143] E. Tchambak. Mitigation of severe slugging using gas injection. *Interim PhD review, Report No. 2, Cranfield University, England*, 2004.

[144] S. Skogestad and I Postlethwaite. *Multivariable Feedback Control: Analysis and Design*. Wiley & Sons, 2005.

[145] S. Skogestad. A Procedure For SISO controllability analysis - with application to design of pH neutralization process. *Computers & Chemical Engineering*, 20(4):373–386, 1996.

[146] J. Chen. Logarithmic integrals, interpolation bounds and performance limitations in mimo feedback systems. *IEEE Transactions on Automatic Control*, 45(6):1098–1115, 2000.

[147] Kemin Zhou, John C. Doyle, and Keith Glover. *Robust and Optimal Control*. Prentice Hall, 1996.

[148] Kemin Zhou and John C. Doyle. *Essentials of Robust Control*. Prentice Hall, 1998.

[149] E. Jahanshahi and S. Skogestad. Closed-loop model identification and pid/pi tuning for robust antislug control. *10th IFAC International Symposium on Dynamics and Control of Process Systems*, pages 233–240, 2013.

ISSN (online): 2246-1248
ISBN (online): 978-87-7112-796-6

AALBORG UNIVERSITY PRESS